Climatic and societal impacts in Scandinavia following the 536/540 CE volcanic double event

Evelien van Dijk[1], Ingar Mørkestøl Gundersen[2], Anna de Bode[3], Helge Høeg[2], Kjetil Loftsgarden[2], Frode Iversen[2], Claudia Timmreck[4], Johann Jungclaus[4] and Kirstin Krüger[1]

1. Department of Geosciences, University of Oslo, Oslo, Norway
2. Museum of Cultural History, University of Oslo, Oslo, Norway
3. Department of Geography, University of Bergen, Bergen, Norway
4. Max Planck Institute for Meteorology, Hamburg, Germany

Correspondence: Evelien van Dijk (e.van.dijk@geo.uio.no), Ingar Mørkestøl Gundersen
10 (i.m.gundersen@khm.uio.no), and Kirstin Krüger (kirstin.kruger@geo.uio.no)

Abstract

In the Northern Hemisphere, the mid-6th century was one of the coldest periods of the last 2000 years, which was initiated by volcanic eruptions in 536 CE and 540 CE. Here, we study the effect of this volcanic double event on the climate and society in Scandinavia with a special focus on
15 Southern Norway. Using an ensemble of Max Planck Institute ESM transient simulations for 521-680 CE, temperature, precipitation and atmospheric circulation patterns are analysed. The simulated cooling magnitude is used as input for a growing degree day (GDD) model set-up for three different study areas in Southern Norway, representative of typical meteorological and landscape conditions. Pollen from bogs inside these study areas are analysed at high resolution (1-3 cm sample intervals)
20 to give insights into the validity of the GDD model set-up with regard to the volcanic climate impact on the regional scale, and to link the different data sets with the archaeological records.
We find that after the 536/540 CE double event, a maximum surface air cooling of up to 3.5 °C during the mean growing season is simulated regionally for Southern Norway. With a scenario cooling of 3 °C, the GDD model indicates crop failures were likely in our northernmost and western
25 study areas, while crops were more likely to mature in the southeastern study area. These results are in agreement with the pollen records from the respective areas. Archaeological excavations show, however, a more complex pattern for the three areas with abandonment of farms, severe social impact but also a continuation of occupation or a mix of those. Finally, we discuss the likely climatic and societal impacts of the 536/540 CE volcanic double event by
30 synthesising the new and available data sets for the whole Scandinavia.

1. Introduction

Large volcanic eruptions are the main driver of natural climate variability in the pre-industrial era of the last millennium (Hegerl et al., 2006). Double eruptions or clusters of eruptions that occurred in the last 2000 years frequently coincide with cold periods in the Northern Hemisphere (NH, Briffa et al., 1998; Zhong et al., 2011; Miller et al., 2012; Sigl et al., 2013). One of the coldest decades in Europe and the NH of the last 2000 years occurred during the mid-6th century, which was initiated by the volcanic double event in 536/540 CE. This cold period was discovered in tree-ring and ice core records (Baillie, 1994; Larsen et al., 2008; Büntgen et al., 2011; Sigl et al., 2015), and coincided with historical documents reporting a dimming of the sun starting in March 536 CE (Stothers and Rampino 1983; Stothers, 1984; Rampino et al., 1988; Kostick and Ludlow, 2015). Updated ice core chronologies reveal two sulphur peaks that correspond to eruptions in 536 CE and 540 CE (Baillie et al., 2008; Sigl et al., 2015). In addition, a third volcanic eruption occurred in 547 CE (Sigl et al., 2015). This event was relatively small compared to the 536 CE and 540 CE eruptions, but it might have aided in the persistence of the cooling after the volcanic double event (Büntgen et al, 2016; Di Cosmo et al., 2017; van Dijk et al., 2022). Tree-ring records from the Alps and Altai recorded a cooling that lasted up to a century following these eruptions, and this period has therefore been named the Late Antiquity Little Ice Age (LALIA, Büntgen et al., 2016), but the extent and duration of the cold period is debated (Helama et al., 2017). Climate model studies indicate a multidecadal cooling rather than a centennial one for the NH, likely impacting society in Scandinavia (Toohey et al., 2016; van Dijk et al., 2022), but the extent of crisis or adaptation by societies in Norway during this time is unknown.

The centuries preceding the first millennium are characterised by great societal changes, including the ending of Antiquity and the beginning of Early Medieval state formations, a process historians believe to have been reinforced by the multidecadal cooling of the 6th century and the outbreak of the Justinian plague in 541 CE (Little, 2006; Rosen, 2006; McCormick et al., 2012). However, less is known about causal relationships between global cooling, regional climate, and local societal changes in Scandinavia.

The 536 CE eruption has been linked to the 'Fimbulwinter myth' (Axboe, 1999; 2005; Gräslund, 2008; Gräslund and Price, 2012), during which no summer occurred for three years in a row. Gräslund and Price (2012) interpret the Fimbulwinter myth as a poetic rendition of a profound social crisis during the 6th century cooling event. A prolonged summer cooling could have potentially led to widespread crop failure. This is especially true for areas that are already at the temperature limit for growing certain crops, where the effect could be substantial. Evidence for reforestation in different parts of central and northern Europe has been associated with significant changes in the archaeological record and what has been termed the 'Migration Period Crisis' (Welinder, 1975; Berglund et al., 1996; Berglund, 2003; Gundersen, 2019). Based on excavations and dating of several sites in central Sweden, Gräslund and Price (2012) even go as far as to assume that the population in present-day Norway and Sweden in the mid-6th century may have declined by half.

Other evidence, however, suggests that there are regional differences in the climatic impact to this cooling (Degroot et al., 2021). Several studies highlight the importance of subsistence strategies

when discussing societal variability to the cooling event. Communities heavily dependent on cultivation are more likely to have experienced an outright crisis, while those predominantly based on wildlife and pastoralism may have been able to adapt (TeBrake, 1978; Verhulst, 2002; Gräslund and Price, 2012; Tvauri, 2014; Hines and Ijssenagger, 2017; Oinonen et al., 2020; Hatlestad et al., 2021). These factors are likely to have contributed to considerable regional diversity in disaster impact (Gundersen, 2021).

In Norway, the mid-6th century is associated with profound changes in social organisation and material culture, which defines the very transition from the Early to the Late Iron Age (500 BCE-550 CE/550-1050 CE). Often understood as a turning point in Norwegian prehistory, many archaeologists discuss a possible causal relationship with the volcanic double event in 536/540 CE (Iversen, 2016; Gundersen, 2019). Bajard et al. (2022) reconstructed agricultural practices from the evidence of lake sediments in southeastern Norway (lake Ljøgottjern) and identified a correlation between temperature change and agricultural practices in this area during the Late Antiquity. This result is supported by the study of ter Schure et al. (2021), where analysis of DNA for the same lake sediment led to the same conclusion. However, the landscape in Norway is very diverse, with coastal areas, mountains, and valleys, leading to differences in regional climate and agricultural practices. Thus, considerable differences in social vulnerability to climate change can be expected throughout the broader study area.

In this study, we follow up on van Dijk et al. (2022), and use the Paleo Model Intercomparison Project phase 4 (PMIP4) past2k and the 6th-7th century Max Planck Institute Earth System Model (MPI-ESM) simulations to analyse the atmospheric circulation and surface climate changes in response to the 536/540 CE eruptions, with a focus on Scandinavia and Southern Norway. Three sites, Fron, Sarpsborg and Høgsfjorden, are selected for case studies with a growing-degree-day (GDD) model, representing different weather and climate regimes and landscapes in Southern Norway. The GDD model utilises the maximum cooling simulated by the MPI-ESM ensemble, and the results are then compared to archaeological and pollen records to shed more light on the climate, vegetation and societal impacts for Southern Norway. We discuss the likely post-volcanic climatic and societal response over Scandinavia based on the climate model data spread, atmospheric circulation patterns, the local archaeology and pollen records in addition to other available records.

2. Methods

2.1 Climate model simulations

The climate model simulations were run with the MPI-ESM1.2-LR, which is the low-resolution (LR) version used for the Coupled Model Intercomparison Project phase 6 (CMIP6) and the PMIP4. This model version has an atmospheric horizontal resolution of 1.9°x1.9°, and 47 vertical layers, with the top at 0.01 hPa (80 km altitude). The ensemble consists of ten 520-680 CE runs (members 1-10), which were branched off from the past2k (#1) in the year 521 CE by perturbing the atmospheric diffusivity, and two 'past2k' runs (two members, hereafter #11 and #12), following the protocol of

Jungclaus et al. (2017). The past2k simulations and the 520-680 CE ensemble are described in more detail by van Dijk et al. (2022). A more complete description of MPI-ESM1.2-LR in its CMIP6 configurations, including parameter and tuning choices, is given in Mauritsen et al. (2019).

115   2 m air temperature, precipitation, and sea level pressure (SLP) anomalies were calculated by subtracting the multiyear monthly mean of the period 1-1850 CE from the past2k run (#1). From these anomalies, the seasonal means for the average growing season in Scandinavia (April to September, hereafter AMJJAS) and the ensemble mean were calculated. For the model runs, only monthly values were archived and are available to this study, and therefore we show the growing season mean for the model simulations. 'Two years after the eruption' therefore means the two

120   growing seasons after the simulated eruption (eruptions are simulated in January). 536-560 CE is taken for the long-term mean, as this is the recovery time after the volcanic double event for temperature. The first two growing seasons after each of the 536 CE and 540 CE eruptions are taken for the short-term response, which is the peak-response time. The significance of the anomalies for the time series was calculated by taking the 2σ (1σ for precipitation) of the control run

125   mean (no volcanic forcing), and the significance for the spatial patterns was calculated by bootstrapping. For this, random 2-year and 25-year periods were taken from the control run to make a time series of 1000 timesteps, which was used to calculate the standard deviation. The 2σ (1σ) was then subtracted from the model ensemble to calculate the significance of the volcanic signal. For more details on this method see van Dijk et al. (2022).

130

The applied GDD model is based on daily mean meteorological observations in Norway from 1961-1990 (Section 2.2). To estimate the relative degree of cooling simulated by the 6th century climate model runs as input for the GDD model, we used an extension of the past2k run (#2) over the historical period (1850-2014 CE). We compare the simulated 1961-1990 mean temperature in the

135   historical run with the meteorological mean temperature anomalies over the study period to calculate the maximum simulated cooling after the 536 CE and 540 CE eruptions compared to 1961-1990 period (Section 3.1; Table 1).

Table 1. Average temperature in Scandinavia for different ensemble members and periods.

Model run	Time period	Average temperature	Difference to 1961-1990
Historical	1961-1990	8.8 °C	-
past2k	1-1850 CE	8.4 °C	-0.4 °C
521-680 ensemble mean	536-560 CE	7.8 °C	-1.0 °C
521-680 ensemble mean	537 CE	7.2 °C	-1.6 °C
521-680 ensemble mean	541 CE	6.7 °C	-2.1 °C
Individual run max cooling	541 CE	5.3 °C	-3.5 °C

2.1.1 Atmospheric circulation analysis

140 During winter to spring, climate in Scandinavia is influenced by four winter atmospheric circulation modes: A positive North Atlantic Oscillation (NAO), a negative NAO, the North Atlantic ridge, and the Scandinavian blocking (Vautard, 1990; Michelangeli et al., 1995; Cassou, 2008). One of the most prominent teleconnection patterns in all seasons is the NAO. The NAO+ is defined as a strengthening of the high pressure centre over the mid-latitudes, generally around Portugal/the

145 Azores, as well as a strengthening of the low pressure centre over Iceland (Hurrell, 1995), which leads to an increased pressure gradient driving a more vigorous westerly jet. The NAO is associated with changes in the location and intensity of the jet stream, as well as the patterns of heat and moisture transport (Hurrell, 1995). These changes affect the temperature and precipitation patterns over Europe and Scandinavia (van Loon and Rogers 1978). The NAO+ brings higher temperatures

150 and increased precipitation over Scandinavia, and the NAO- brings lower temperatures and decreased precipitation. The North Atlantic ridge is associated with a high pressure over the Atlantic and a low pressure over Scandinavia, leading to colder and wetter conditions over Northern Europe. The Scandinavian blocking is represented by a stable high pressure system over Scandinavia, resulting in warm and sunny conditions over this region (Cassou, 2008; Tedesco, 2020).

155 Atmospheric circulation patterns can be obtained by using empirical orthogonal function calculations and projecting the first 4 modes on the SLP fields (Hurrell, 1995). The empirical orthogonal function extracts the most occurring pattern from a data set over time. In this study, the simulated monthly mean SLP from the past2k run #1 is used to calculate the different modes for 1-1850 CE. The SLP anomaly patterns are then compared to the four most commonly identified patterns from this EOF

160 analysis.

2.2 Growing degree day modelling

'Growing degree days' is defined as the accumulated daily mean temperature sum during the growing season, where the growing season is the period with daily mean temperatures at or above 5 °C (Fig. 1c, Carter, 1998; Hanssen-Bauer et al., 2017). Local GDD values can then be calculated by

165 using local weather data, which is projected on a terrain model in a geographical information system (ArcGIS) by using a lapse rate of minus 0.6 °C for every 100 masl (McIlveen, 1986; Stamnes, 2016; Strand, 1984). Mean daily temperature observations from the Norwegian Meteorological Institute for the standard climate period of 1961-90 are used as baseline values (https://www.met.no/en/free-meteorological-data/Download-services). Grain species have different GDD requirements for

170 reaching maturity, depending on local climate and topographical conditions (Frøseth, 2004; Strand, 1984). In pre-modern times, barley had a basic requirement of approximately 1200-1350 GDD, oats needed 1300-1350 GDD, rye 1100 GDD, and wheat 1550 GDD (Foss, 1926). Barley and oats could be sown in either early or late spring, resulting in a wider range of GDD requirements than for rye and wheat. These values must be recalculated for each area in question according to the number of

175 solar hours and precipitation during summertime. Due to the greater number of solar hours in northern areas, the required heat budget decreases with approximately 20 GDD per degree of latitude north of 60 ºN (Frøseth, 2004; Strand, 1984; Åssveen & Abrahamsen, 1999). Rainfall

exceeding 250 mm from May to August increase the required temperatures with an additional 60-80 GDD per 100 mm rainfall for barley, 90-100 mm for oats, and 100-110 mm for wheat (Frøseth, 2004).

180 The three case study areas are *Fron,* located in the Gudbrandsdalen valley (eastern inland Norway), *Høgsfjorden*, located in Rogaland (southwestern Norway), and *Sarpsborg,* located on the eastern side of the Oslo fjord (southeastern Norway, Fig. 1a). The three areas represent three different weather and climate regimes in Southern Norway (Figs. 1 b-c). Several archaeological excavations and field studies have been carried out in these areas (Section 2.3), including pollen analysis from

185 sediment cores with high resolution (Section 2.4). This provides a thorough cultural historical context against which to analyse and compare the different GDD model output.
By taking the factors described above into consideration, the local requirements for the three study areas can be defined (Table 2; Gundersen, 2021).

190 **Table 2. Information about the three different sites for the growing degree day modelling, based on local growth conditions and 1961-90 meteorological data for each area.**

Area	Mean summer precipitation	Latitude	Barley requirements	Rye requirements	Oats requirements	Wheat requirements
Fron	230 mm	61.5 °N	1169-1319 GDD	1069 GDD	1269-1319 GDD	1519 GDD
Høgsfjorden	434 mm	58.8 °N	1351-1501 GDD	1123 GDD	1497-1547 GDD	1766 GDD
Sarpsborg	277 mm	59.2 °N	1234-1384 GDD	1115 GDD	1341-1391 GDD	1594 GDD

In this study, two definitions for growing season are used. For the MPI-ESM simulations, monthly mean data are available to create a *mean* growing season, where the months April to September are taken. The definition of the actual growing season, however, is the number of days with a temperature at or above 5 °C, which can be different from year to year. This is referred to as the

195 *active* growing season (Carter, 1998).

2.3 Archaeological setting, data, and study areas

The three selected study areas were parts of larger 'tribal' areas in the Roman and Migration periods (200–550 CE). 1500 years ago, the Scandza peninsula, which included present-day Sweden and Norway, was home to at least 25 tribal communities. According to the learned Greek author

200 Procopius (1919 [~530-560], Book XIV and XV), there were 'thirteen very numerous nations' (nationes) in Thoulē (which equates to Scandza), one of which was probably the people Heiner (heiðnir) of Hedmark that the Fron area probably belonged to (Iversen, 2019). The peoples of

Vikverir held land in the historic region Viken, where the lost Medieval country Vingulmark contains the Sarpsborg area, while the Høgsfjorden area was located among the people of Rugi in Rogaland. Over the next 500 years, these 'numerous nations' united into two larger kingdoms: Norway and Sweden (Brink, 2008a; Andersson, 2009; Iversen, 2019). This political process is intimately associated with the 5th-6th centuries CE, during which time there was a distinct turn towards ideas of kingship and political centralisation (Skre, 2019). This development is usually understood as a response to the political and social turmoil of the Migration Period (400-550 CE), in which climate deterioration and social unrest may have been contributing causes (Iversen, 2016; Skre, 2019).

Fron area

Fron is is the northernmost of our case study areas, and it is located in the narrow Gudbrandsdalen valley (Fig. 1a). In the Middle Ages, Fron was part of the þriðjung (legal district) of Søndre Gudbrandsdalen (Fig. 1a), which borders the þriðjung Nordre Gudbrandsdalen to the north and þriðjung Hedmark and Østerdalen to the south. These three legal districts had a common popular thing (legal assembly) at Åker, which may reflect the pre-state Iron Age political autonomy of the Heiner tribe (Iversen and Brendalsmo, 2020; Iversen, 2021). Archaeological excavations testify to permanently settled farming communities in Fron from around 1000 BCE that based their economy on a combination of outfield exploitation, husbandry and crops (Gundersen, 2016). Husbandry, including extensive grazing in the lower mountain areas, has traditionally constituted an important part of the farming strategies in the valley (Gundersen, 2021). Although considered fertile, the agricultural lands are restricted by topography and considered marginal in agricultural terms (Puschmann, 2005). This area has a lower accumulated growing degree count for the growing season compared to the other two areas, and the lowest summer precipitation of the study areas. The local wind direction is dependent on the valley orientation, which is east-west, leading to a prevailing wind from the west (Fig. A5a). The bog located in this area is Ulbergmyr and is further described in Section 2.4 (Fig. 1a).

Høgsfjorden area

The Høgsfjorden is the westernmost of our research areas and is located east in the county of Rogaland. The name Rogaland derives from 'Rugi', meaning the 'rye-growers', which is mentioned as one of the Scandinavian tribal groups in contemporary written sources (Brink, 2008; Malone, 1962; Neidorf, 2013). Judging from the number of burials, the Rugi may have been one of the most populous tribes in present-day Norway in the Iron Age (Iversen, 2019). Rogaland is a highly diversified landscape, characterised by areas with wide-stretching agricultural landscapes along the coast, cultivated narrow valleys and pastured heaths in the surroundings, but situated in an otherwise mountainous, rough, and infertile fjord landscape (Puschmann, 2005). As such, the preconditions for agriculture differ considerably within the region.

This area has a similar length of growing season as the Sarpsborg area, but higher summer precipitation, which leads to higher growing degree days requirements for crops (Figs. 1b-c, Table 2). The annual mean wind direction is from the west. Because of the fjords, the local wind direction is directed by the shape and orientation of the valley. For the Forsand valley, where the excavation sites and the bog are, this means the wind comes from the southwest or the northeast. No meteorological station is available for this fjord, so data has been taken from a nearby valley with a

similar orientation (Fig. A5c). Forsand is characterised by poor agricultural soils surrounded by steep
mountains, but the excavations have nonetheless provided evidence for large continuous farming
settlements all the way back to ~1500 BCE (Løken, 2020; Westling et al., 2022). However, long-term
overexploitation led to soil deterioration, which ultimately made necessary changes in subsistence
strategies (Løken, 2020). Oats, which thrive even with poor soils, became more important, as well as
husbandry and grazing. According to Westling et al. (2022), the population at Forsand eventually
became larger than what could be sustained by local food production alone. Wool from sheep/goats
appears to have become an important part of their economy and used in exchange for food imports.
Thus, the community also became vulnerable to trade disruptions and poor harvests - both domestic
and among their trading partners. The bog in this area is Åsheimmyr (Fig. 1a, Section 2.4)

Sarpsborg area

Sarpsborg is the easternmost of our research areas (Fig. 1a) and is located south in the medieval
county of Vingulmark, which included the coastal land from Sweden to Vestfold. To the east,
Vingulmark bordered Ranrike (Båhuslen) and Värmland, to the north to Romerike, Ringerike and
Numedal, and to the west extended to Vestfold (Munch, 1849). In the Iron Age, the area may have
been inhabited by a group referred to as the Lidvikinger (Lidwicingum) (Iversen, 2019). The area is
highly fertile and one of the most cultivated landscapes in present-day Norway (Puschmann, 2005).
Hence, Sarpsborg and surrounding areas have provided archaeological evidence for well-developed
farming communities as early as the late Neolithic (~2350-1800 BCE) (Bårdseth, 2008; Damlien et
al., 2021). Prehistoric farms, including from the Iron Age, have mostly been found on the fertile
terminal moraines that offered excellent conditions for cultivation. Although the outfields and marine
resources are considered to have been of some importance for the early farmers, the location of the
settlements is mostly understood in terms of farming in general and crop production in particular (cf.
Bårdseth, 2008). Thus, the importance of crops for nutrition appears to have been greater than in
Fron.

This area has quite high accumulated temperature for the growing season, and has the second
lowest summer precipitation of all three case studies (Figs. 1b-c). The wind direction is mainly from
the south or west, but because this area is flat, it is more variable than for the other two case study
areas, as the wind direction is not confined by the topography (Fig. A5b). The bog used for the pollen
analysis in this area is Haraldstadmyr (Fig. 1a, Section 2.4).

The length of the active growing season (based on 1961-1990 data) for the three different case
study areas is shown in Fig. 1c. From this map, we can see that the growing season is the longest at
the coast, and shortest in the inland valleys of Southern Norway.

2.3.1 C14 data

The collected radiocarbon dates come from different contexts, such as buildings, clearance cairns,
agricultural layers and a variety of other activities. The data also includes dates from exploitation of
outfield resources. However, iron and charcoal production sites are excluded from the C14 data.
Data from these sites may skew the data as most of these production sites are from 900–1300 CE
and almost exclusively from certain inland regions (Loftsgarden 2020). Likewise, we have omitted
dates from cooking pits, as they represent a temporally restricted cultural phenomenon in Norwegian

archaeology (Gundersen, Rødsrud, & Post-Melbye, 2020). They are mostly associated with the Early Iron Age (500 BCE-550 CE) and frequently used for dating purposes, thus creating an overrepresentation of Early Iron Age dates in the overall record.

To model the C14 dates, we have used the Summed Probability Distributions (SPD) analysis within the rcarbon package (Crema and Bevan 2020) in the R statistical programming language (R Core Team, 2019). Dates were calibrated using the Intcal20 calibration curve (Reimer et al., 2020). All dates are presented as calibrated dates BCE/CE.

Well-researched areas and well-dated sites can potentially cause the SPDs to be biased and might generate misleading peaks in the SPD. To mitigate this effect we have implemented artificial bins in rcarbon. We have structured the dates into bins at the site level, with a cut-off value at 50 years, prior to the SPD analysis. This method and data are further described by Loftsgarden and Solheim (in press).

285

290

295
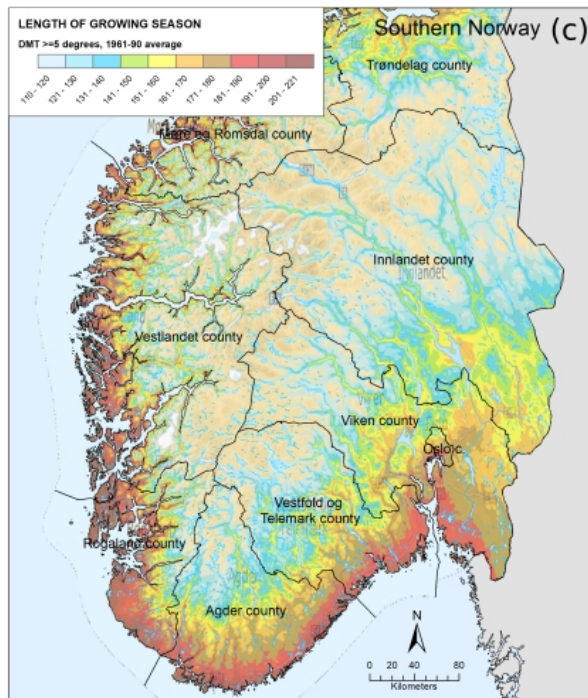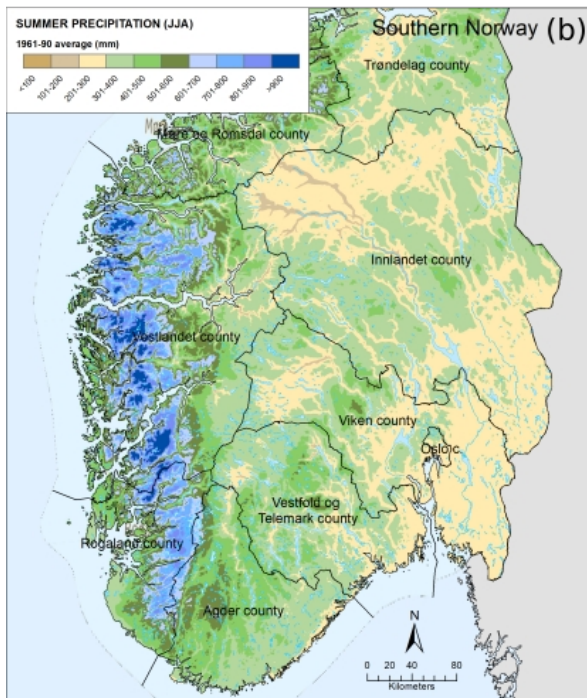
Figure 1. a) The three case study areas and associated sites. Red outline indicates the regions, bold names are the areas and the stars indicate the locations and names of the bogs analysed for pollen. DEM map from ESRI 2020. b) The summer precipitation and c) average length of the growing season (days) for Southern Norway during 1961-1990, for days with a daily mean temperature (DMT) at or above 5 °C (adapted from Hanssen-Bauer et al., 2017).

300

2.4 Pollen analysis

Pollen analyses were carried out on material from three different peat bogs in Haraldstadmyr, Ulbergmyr and Åsheimmyr (Table 3). The cores were sampled with a Russian corer from the deepest parts of the bogs (Høeg, 1999; de Bode, 2021; and Gundersen, 2021).

Bulk samples for radiocarbon dating were dated by Lund University Radiocarbon Dating Laboratory and Tandem Laboratory at Uppsala University, and calibrated using the IntCal20 calibration curve (Reimer et al., 2020). The age-depth model was generated using R software and the R code package 'Bacon' 2.4.3 (Blaauw and Christen, 2011).

Approximately 1 cm^3 of peat was collected for each pollen sample, at intervals varying from 1 cm to 20 cm. For each peat sequence, 1-3 cm intervals (~8-24 years resolution) were used for the depths corresponding to the time period 250-1150 CE in order to obtain a high resolution palynology. Pollen percentages were calculated based on the pollen sum (ΣP), which expresses the total terrestrial pollen taxa. Percentages of the local and aquatic pollen types, as well as most of the spore plants and the number of charcoals, were calculated based on ΣP+X, where X represents the pollen type, spore or charcoal in question.
Pollen diagrams were plotted using R version 4.0.3 (2020-10-10) with the packages 'rioja' version 0.9-26 (Juggins 2020), 'ggplot2' version 3.3.3 (Wickham 2016), 'tidyverse' version 1.3.0 (Wickham et al., 2019) and 'neotoma' version 1.7.4 (Goring et al., 2015). The pollen percentages were plotted against their corresponding mean ages as generated by the age-depth model (Section C in the Appendix).

Table 3. Information about the three peat sequences collected for pollen analysis.

Site name	Date of coring	Coordinates location	Altitude (m.a.s.l.)	Depth (cm)	Sample intervals (cm)	Resolution (yrs)	No. of samples
Ulbergmyr (Fron area)	June 2019	61°33' 4.6"N, 9°54' 36.4"E	275	0-495	Varying from 1-10. For depths 25-130: 1-3.	For depths 25-130 cm: c. 8-24	83
Åsheimmyr (Høgsfjorden area)	June 1982	58°54' 4.7"N, 6°7' 17.7"E	115	30-950	Varying from 2-10. For depths 240-416: 2.	For depths 240-416 cm: c. 13	165
Haraldstadmyr (Sarpsborg area)	May 2018	59°17'42.1"N, 11°03'18.3"E	42	0-282	Varying from 1-20. For depths 80-126: 1.	For depths 80-126 cm: c. 14	82

3. Results

3.1 6th century climate

325 In this section, the results are given for the simulated 6th century climate response to the volcanic double event of 536/540 CE, where the focus is on the mean response for the growing season (AMJJAS) in Scandinavia. To gain insight into the relationship between the volcanic atmospheric impact and the surface climate response, the NH extratropical aerosol optical depth (AOD, Toohey and Sigl, 2017) is shown for the study period. Four large eruptions in 536 CE, 540 CE, 574 CE, and
330 626 CE are visible as large peaks, indicating a more opaque sky (Fig. 2a). The climate model simulations reveal a widespread cooling for the growing season after the 536 CE and 540 CE eruptions in the NH extratropics, which results in an ensemble mean cooling of about 2 °C (Fig. 2b). This cooling remains significant for 10 years after the 540 CE eruption, with a return to the mean temperature from ~555 CE onwards. Temperatures for Scandinavia show a maximum cooling of
335 ~1.5 °C after the 536 CE and 540 CE eruptions, but also a larger internal variability of 1.2 °C compared to 0.4 °C for the NH extratropical mean. This leads to a less distinct volcanic signal. Only the first year after the eruptions is the ensemble mean 2m air temperature outside the range of internal variability, whereas it takes up to 20 years (until 560 CE) for the temperature to return to the mean value (Fig. 2c).

340 For the NH extratropics, precipitation decreases after the volcanic double event by 3 mm month^{-1} (Fig. 2d), which is a significant reduction (on the 1σ level). For Scandinavia, this is up to 7 mm month^{-1}. However, just as with temperature, the volcanic signal on precipitation is only significant right after the eruptions due to high internal variability over Scandinavia (Fig. 2e). After the 540 CE eruption, it takes approximately ten years for the precipitation anomaly to return to 0.

345 During the maximum volcanically induced cooling over Scandinavia, the ensemble mean growing season temperature decreases to the absolute value of 6.9 °C. However, this is the ensemble mean for the whole of Scandinavia. To gain insight into the regional response, we analyse the spatial temperature and precipitation distribution after the volcanic double event for both the long-term and the short-term response.
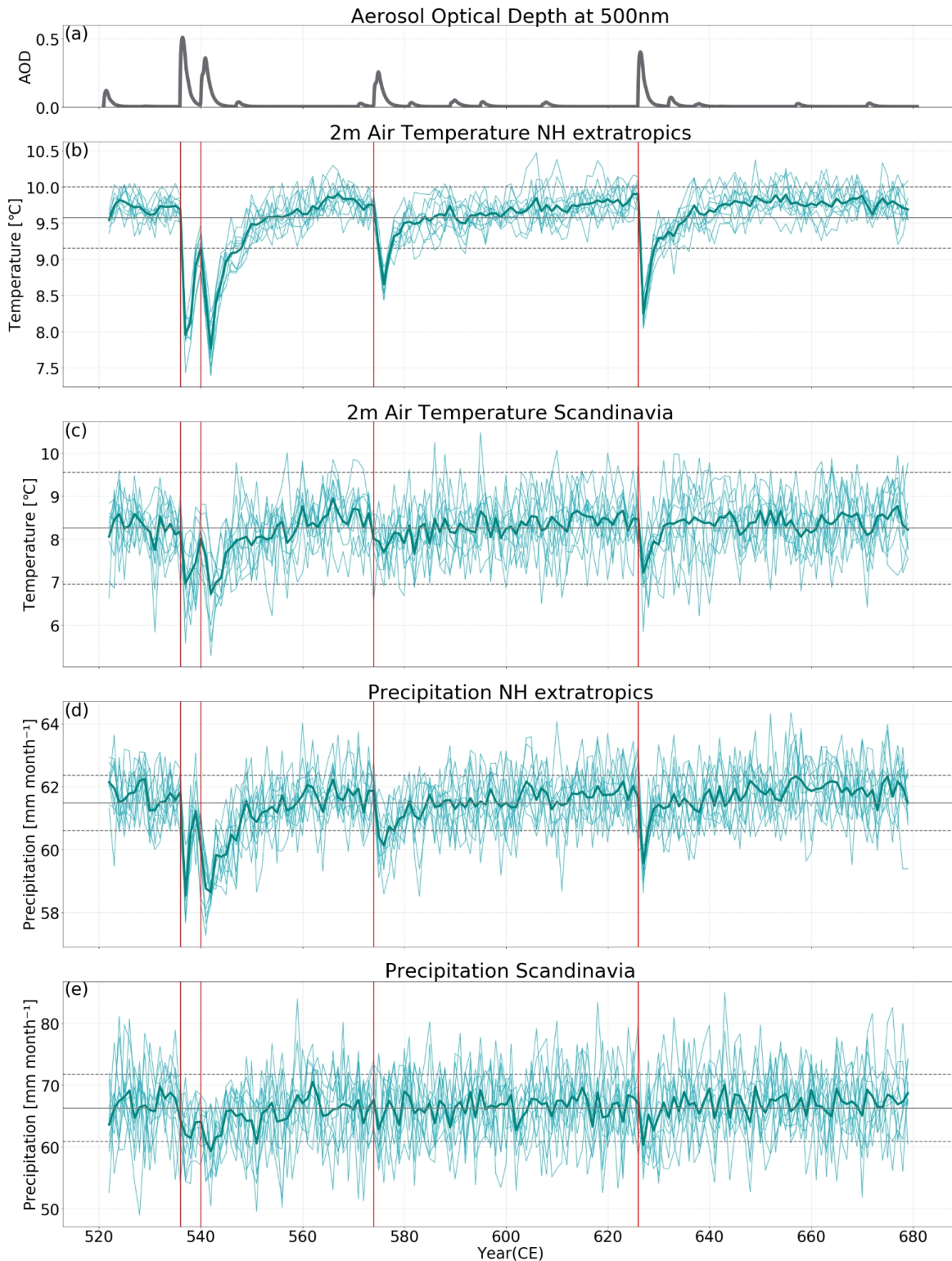
Figure 2. Time series of a) yearly mean NH extratropical (30°-90°N) AOD (Toohey and Sigl, 2017), and growing season (AMJJAS) mean of b) NH extratropical and c) Scandinavian (0°-20°E, 55°-73°N) 2m air temperature, and d) NH extratropical and e) Scandinavian precipitation. Red vertical lines indicate the four large eruptions in the study period. Grey lines indicate the 1-1850 CE mean and the dashed lines the 1σ (2σ) of the control run for precipitation (temperature).

355 The simulated temperature anomaly shows a significant cold period for 25 years after the 536 CE eruption for most of Norway (Fig. 3a). A significant cooling of up to 2 °C occurs in the first two years after the 536 CE eruption (Fig. 3b) and up to 1.5 °C after the 540 CE eruption (Fig. 3c). Overall, the 5 °C line (referring to the 5°C mean for AMJJAS here) shifts south by ~6° in latitude in the first two years after the 536 CE and 540 CE eruptions. The simulated average growing season temperature

360 thus drops below 5 °C for the northernmost study area site (Fron).

Besides temperature, summer precipitation also impacts the harvest. The ensemble mean indicates a drying during the growing season almost everywhere in Scandinavia. A significant drying of up to 5 mm month^{-1} occurs over entire Scandinavia for the 25-year mean after 536/540 CE (1σ, Fig. 3d). For the 2-year mean, a significant reduction of up to 15 mm month^{-1} (15%) occurs after the 536 CE

365 eruption (Fig. 3e), and up to 20 mm month^{-1} (20 %) after the 540 CE eruption in southeastern Norway (Fig. 3f).

The climate over Scandinavia is influenced by large-scale atmospheric circulation patterns with the positive NAO circulation pattern occurring most often during NH winter. This has been shown from observations (1949-1992, Michelangeli et al., 1995), reanalysis data (1974-2007, Cassou, 2008),

370 and also for our past2k climate model simulations (1-1850 CE, Fig. A4a and Section 2.1.1 this study; van Dijk et al., 2022). The NAO+ is also the dominant mode during the growing season (AMJJAS; Fig. A4b). After the 536 CE and 540 CE eruptions, the overall large-scale atmospheric circulation pattern shifts to a higher pressure over the high-latitudes and decreased pressure over the mid-latitudes, over the North Atlantic region (Fig. 4). This corresponds to a shift towards a more negative

375 NAO. 25 years after the 536 CE eruption, the SLP has significantly increased over Scandinavia (Fig. 4a). In contrast, the SLP change 2 years after the eruptions is not significant over Scandinavia (Figs. 4b-c), which could be due to contrasting signals in the first and second year after the eruptions.
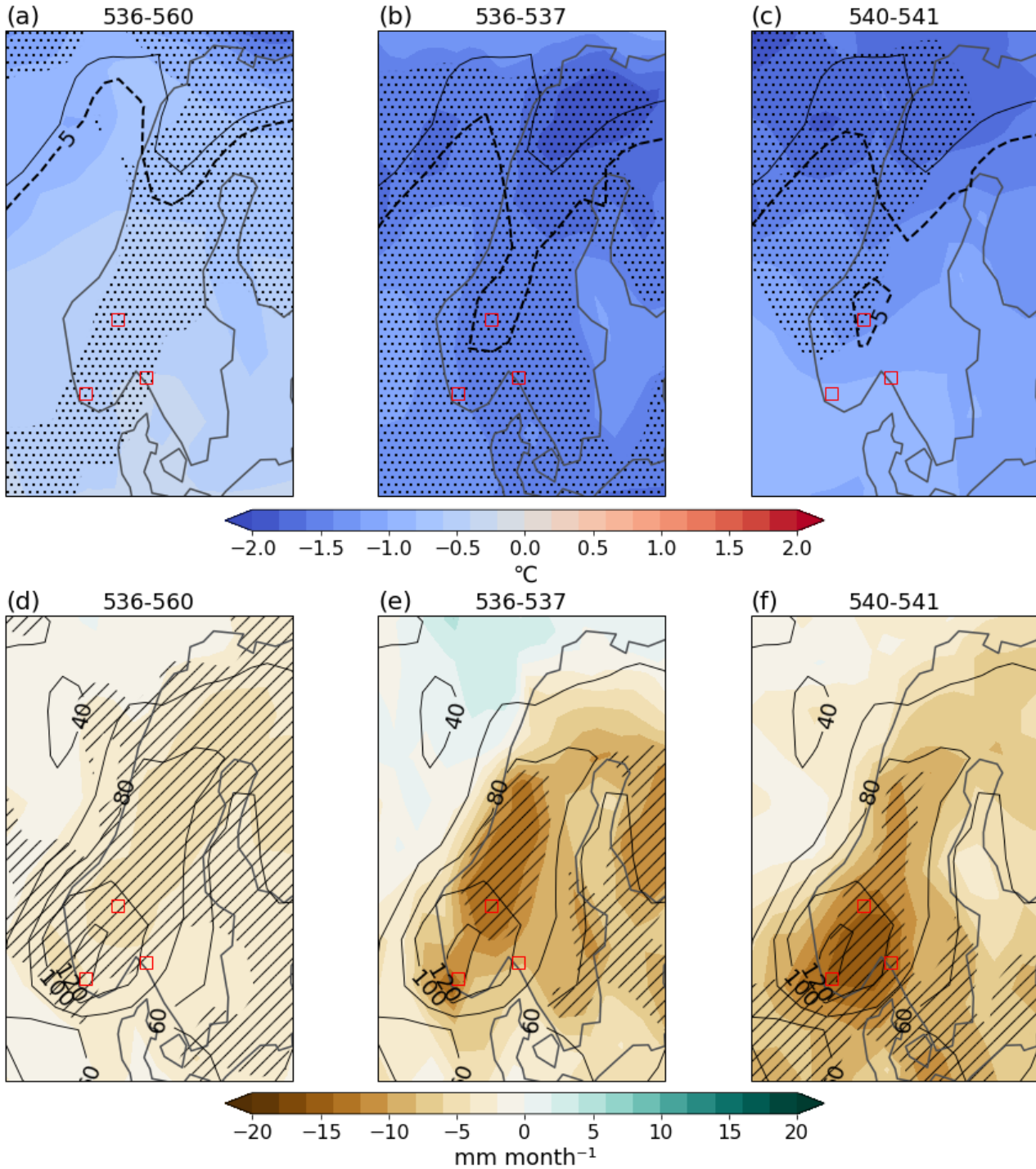
Figure 3. Maps of 2m air temperature (a-c) and precipitation (d-f) anomalies for the mean growing season (AMJJAS) in Scandinavia for 536-560 CE, 536/537 CE, and 540/541 CE. Anomalies are calculated with respect to 1-1850 CE climatology, which is given in contours. The red squares indicate the locations of the local sites used for the GDD modelling. For temperature, the absolute 5 °C line is given by the black dashed and solid contour lines representing the model experiments and climatology respectively. The 1σ (2σ) significant areas are hashed (stippled) for precipitation (2m air temperature).
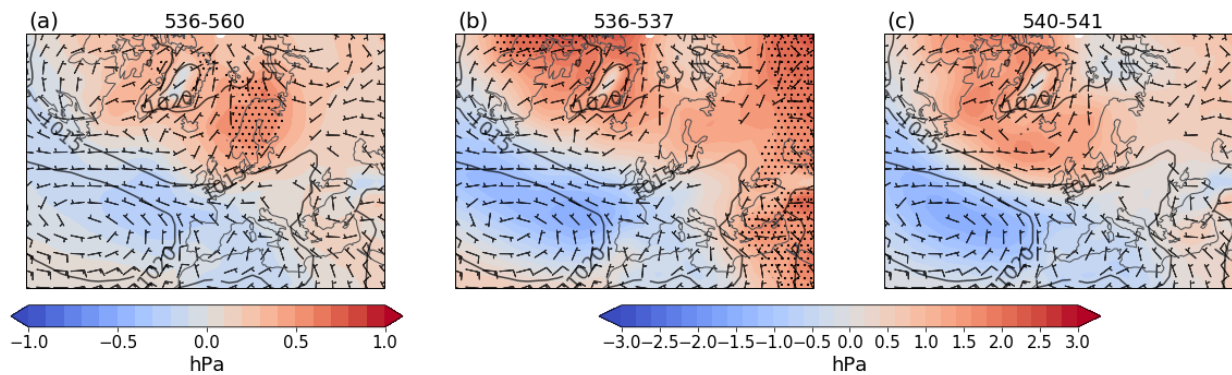
Figure 4. Maps of the North Atlantic ensemble mean sea level pressure anomalies and absolute wind for the mean growing season (AMJJAS) for a) 536-560 CE, b) 536-537 CE, and c) 540-541 CE. Anomalies are calculated with respect to 1-1850 CE climatology, which is given in contours (5 hPa interval). The 2σ significant areas are stippled. Wind barbs are shown for 1, 5, and 10 m/s intervals.

Each individual ensemble run is a possible realisation of the modelled volcanic impact. Therefore, we want to investigate the range exhibited by the individual runs, including the maximum cooling, and hydrological effect after the eruptions. Interestingly, the temperature anomaly for the 25-year mean growing season reveals a significant cooling from 0.8 to ~1.5 °C for half of the runs, whereas the other half shows a non-significant cooling or even a slight warming over Scandinavia (Fig. 5a). Even more striking is, that the 25-year mean precipitation anomalies reveal three ensemble members (ensemble member #3, #5 and #11) that show significant wetting over parts of Scandinavia, whereas the other members (9 out of 12) show drying over the entirety of Scandinavia (Fig. 5b).

Inspecting the first and second growing seasons after the 536 CE and 540 CE eruptions (Figs. A1 and A2), reveals a maximum cooling of close to 3.6 °C for local areas in Norway. There is an even larger spread in the individual simulations for the precipitation anomalies over Scandinavia, compared to the 25-year mean anomalies.

The SLP anomaly maps for the 536-560 CE mean (Fig. 6) reveal eight ensemble members with a significant shift towards higher pressure over the North Atlantic (#5, #7-9, and #12) and Scandinavia (#1-2, and #6), reflecting a weakening of the SLP gradient (the low pressure system over Iceland gets weaker). The remaining four ensemble members hardly show any significant patterns in atmospheric circulation response.
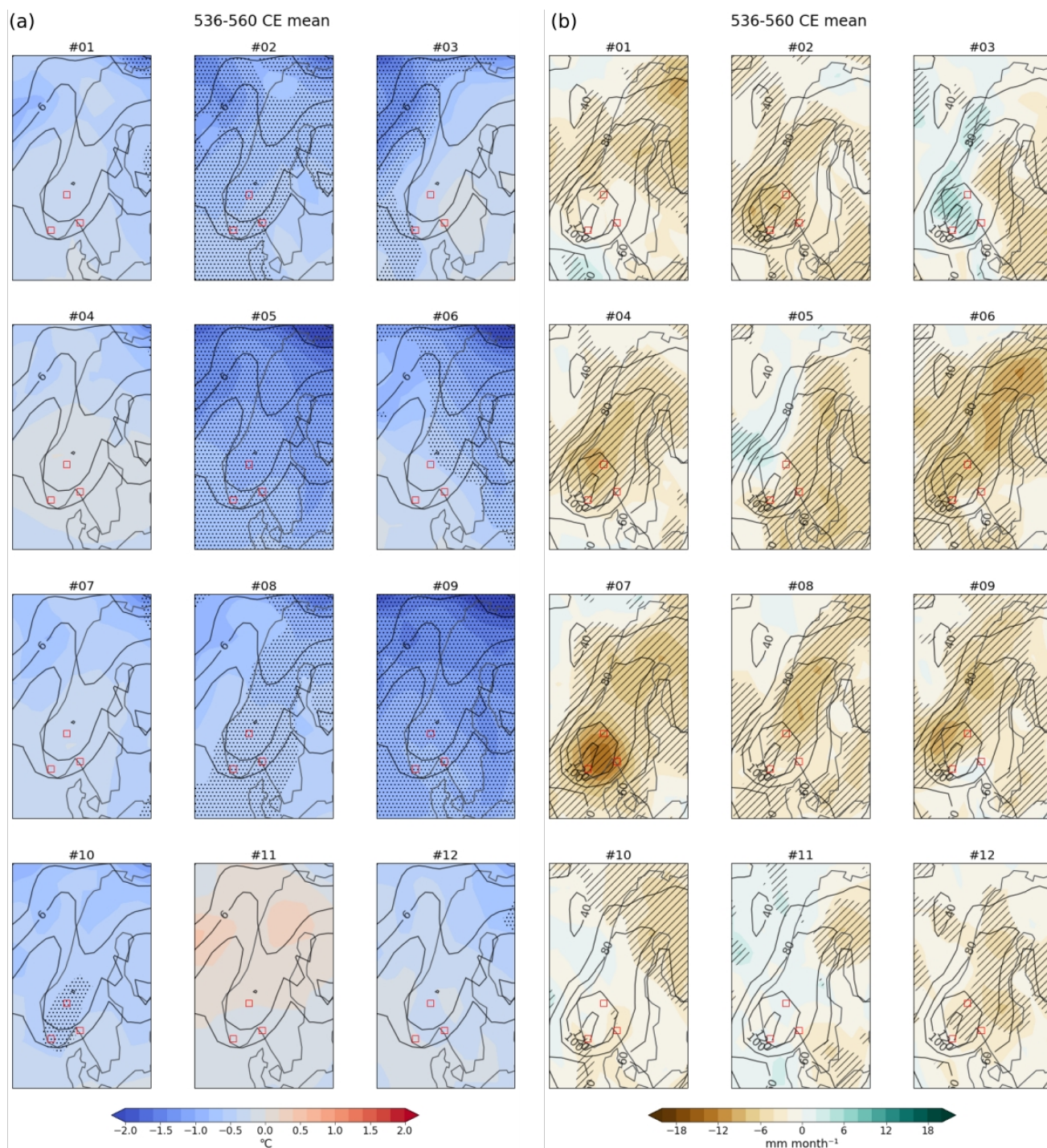
Figure 5. a) temperature and b) precipitation anomaly maps for the mean growing season (536-560 CE) for the individual ensemble members. Anomalies are calculated with respect to 1-1850 CE climatology, which is given in contours. The red squares indicate the locations of the local sites used for the GDD modelling. The 1σ (2σ) significant areas are hashed (stippled) for precipitation (2m air temperature).
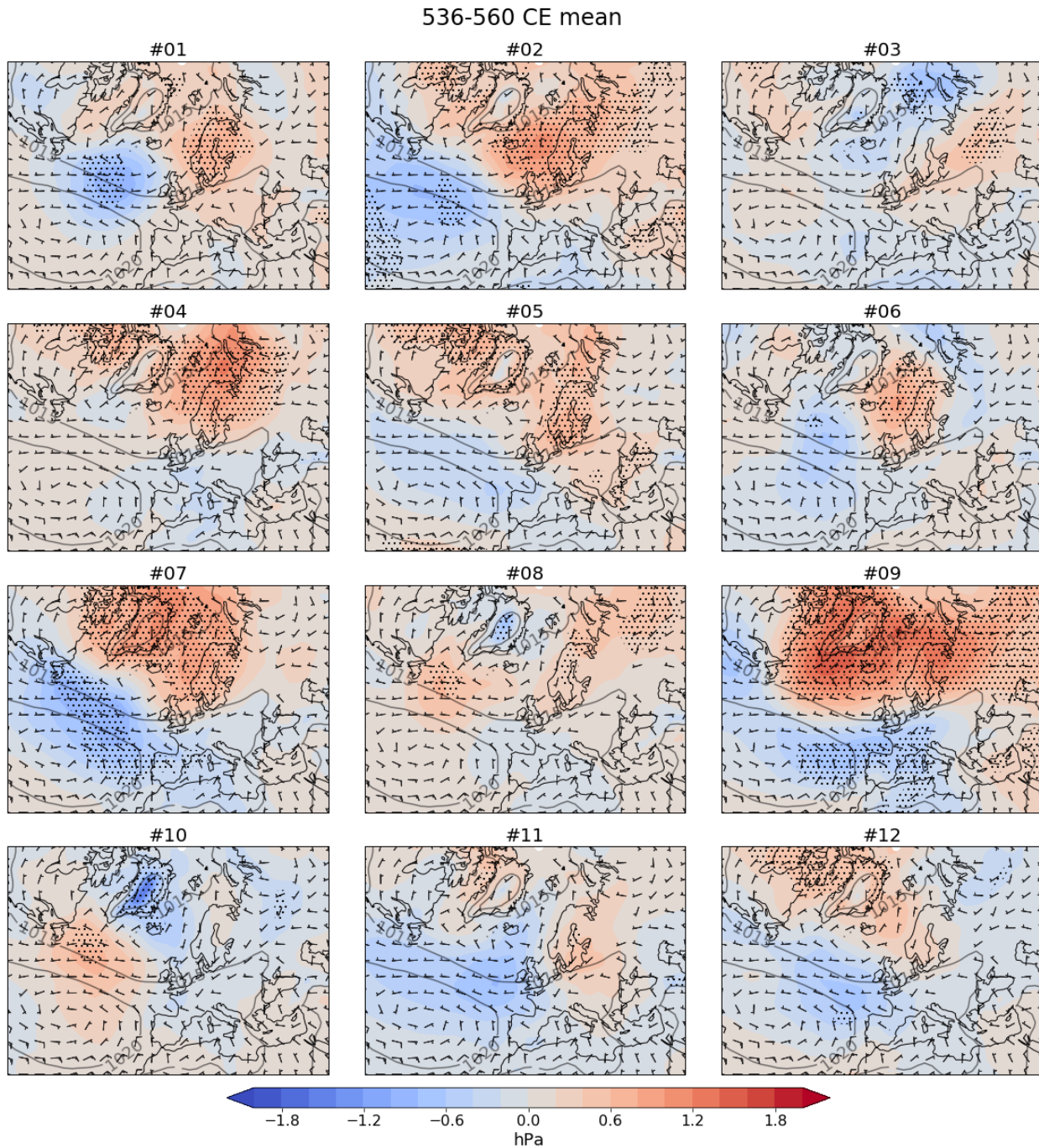
Figure 6. SLP anomaly and absolute 10 m wind maps for the mean growing season for 536-560 CE for the individual ensemble members. Anomalies are calculated with respect to 1-1850 CE climatology, which is given in contours. The 2σ significant areas are stippled. Wind barbs are shown for 1, 5 and 10 m/s intervals.

3.2 GDD model results

415 The average ensemble mean peak cooling in the two years after the 536/540 CE eruptions is 1.6 °C with respect to the 1-1850 CE mean of the past2k run. Recalculating for a reference period of 1961-1990 mean of the historical run (Table 1) leads to an overall 2.1 °C cooling over Scandinavia. However, individual members reveal a significant maximum cooling after the 536/540 CE up to 3.5 °C over Scandinavia, and a maximum cooling of ~3 °C for Southern Norway (Table 1, Fig. A1). To
420 assess the potential impacts on agriculture for the worst case volcanic climate scenario, we apply a 3 °C cooling in the case study areas for the GDD model set up for 1961-1990 climatological conditions (Fig. 7).

Fron, the northernmost of our case study sites in Southern Norway, is situated in a narrow valley. From the map in Fig. 7a and b, it becomes clear that with a 3 °C cooling, the accumulated
425 temperature ends up in the 1100-1300 GDD bin for most of the main cultivated area, but with the remaining areas below 1100 GDD. This means that the minimum requirements for crops to grow (Table 2) are only met for rye and barley in the most favourable areas. However, with small margins to allow for climate variations, harvests are likely to fail or be very small even for these species. This area is thus vulnerable to volcanic cooling.

430 With a 3 °C cooling, the accumulated temperature for Høgsfjorden, located at the southwestern coast of Norway, is around 1400-1700 GDD for the cultivated areas (Figs. 7c,d). This indicates that the minimum requirements are met for rye, barley, and oats, but lower yields can nonetheless be expected for barley and oats. In certain areas, oats may not mature and harvests even fail.

Sarpsborg, located on the eastern side of the Oslo fjord in the southeast of Norway, is a bit warmer
435 than the other two areas, with 1600-1700 accumulated degrees in the growing season after a 3 °C cooling (Figs. 7e-f). Because of low summer precipitation, this means that none of the cereal types appear directly threatened by a cooling event.
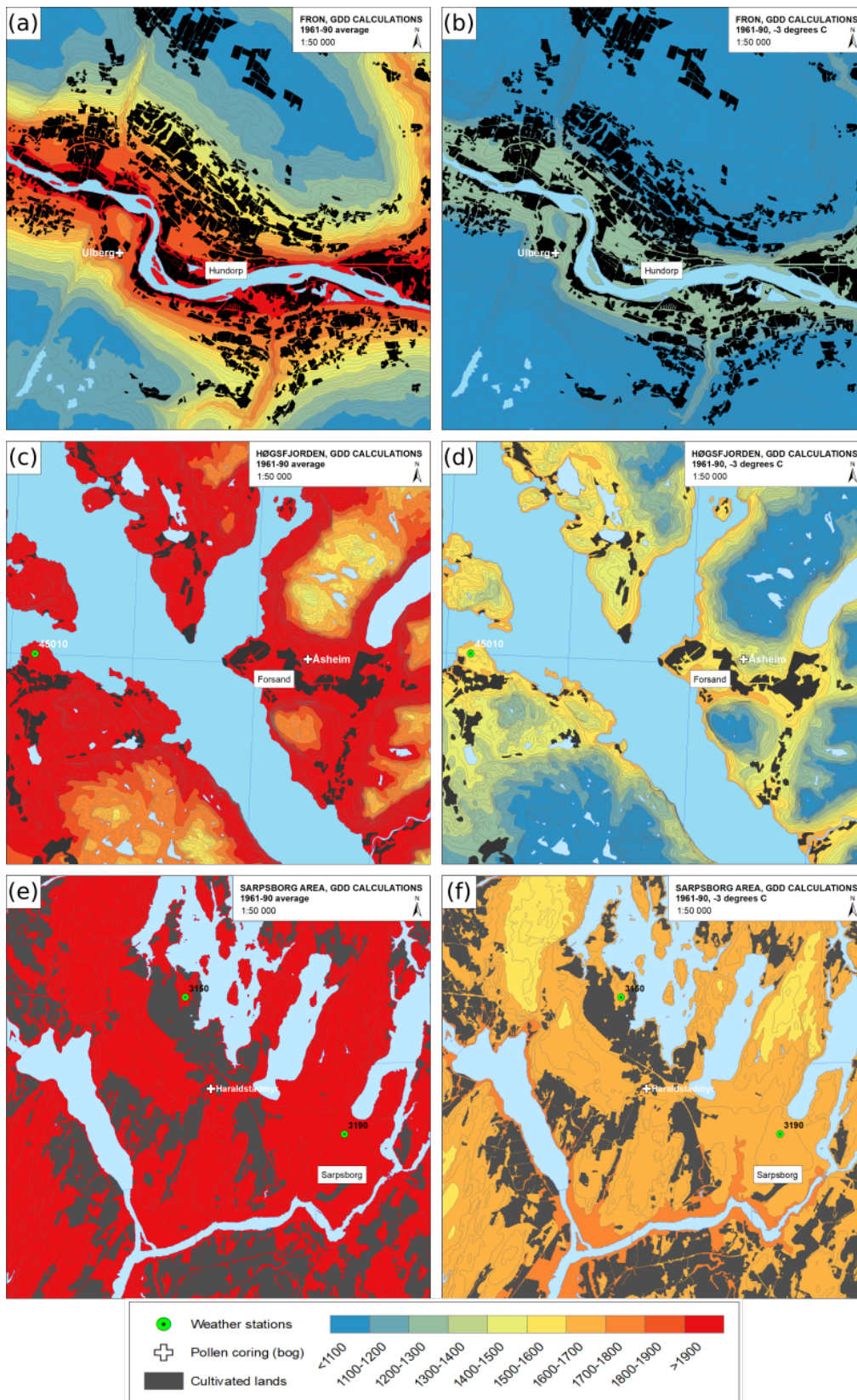
Figure. 7. Growing degree day maps for 1961-1990 for a) Fron, c) Høgsfjorden and e) Sarpsborg and with a 3 °C cooling compared to the 1961-1990 mean for b) Fron, d) Høgsfjorden and f) Sarpsborg.

3.3 Pollen results

The pollen diagrams (Fig. 8) show the transitions in the vegetation of the three selected area's through time, from ca. 250-1150 CE. The time period from 500-600 CE is marked in each diagram. The total number of pollen (ΣP) is depicted on the uppermost axis. The sum fraction of anthropochores is based on the sum of terrestrial pollen of cultivated taxa that are direct indicators of cultivation (Behre, 1981). These include the four cereals *Secale* (rye), *Avena* (oats), *Triticum* (wheat) and *Hordeum* (barley). The sum fraction of apophytes, plotted on the same axis, is based on the sum of terrestrial pollen of ruderal taxa, which serve as indirect indicators for farming practises; specifically grazing activities (Behre 1981). These include *Rumex* (docks and sorrels)*, Rumex longifolius* (northern dock)*, Artemisia* (mugwort)*, Chenopodiaceae* (goosefoot)*, Urtica* (common nettle)*, Plantago major* (common plantain) and *Plantago lanceolata* (ribwort plantain)*.* The fungi of *Sordaria* are plotted on a separate axis. Fungi of *Sordaria* can also indicate the presence of animals and thus serve as an indicator for grazing activities (van Geel, 2003; Cugny et al., 2010; Etienne et al., 2013; Bajard, 2022). In Figs. A9-A11 extended pollen diagrams are given, outlining the individual taxa of the selected apophytes and trees.

The pollen diagram from the Ulberg bog in the Fron area (Fig. 8a) indicates a decrease in both pollen from the anthropochores taxa as well as pollen from the apophytes taxa during 500-550 CE. Studying the individual species reveals that pollen from *Hordeum* (barley) and *Triticum* (wheat) are less abundant around 500-550 CE, coinciding with a decline in charcoal percentages and an increase in tree pollen. Pollen of *Avena* (oats), in juxtaposition, increase during 500-550 CE. Fungi of *Sordaria* remains absent during this time interval. This early 6th century decline is followed by a slight increase again towards the end of the century, and an almost halt to agricultural activities in the 7th century.

In the pollen diagram for Åsheim in the Høgsfjorden area (Fig. 8b), a sharp decline in both the anthropochores and apophytes fractions are noticeable slightly before 550 CE, reaching values as low as 0% around 550 CE. This decline is marked by the coinciding disappearance of pollen from *Avena* (oats), *Secale* (rye), *Triticum* (wheat), as well as an absence of fungi from *Sordaria*. Simultaneously, the total number of pollen decreases. After 550 CE, a drop in charcoal and a gradual increase in pollen of trees can be seen. Percentages of *Hordeum* (barley) vary throughout the 6th century, indicating irregular cultivation of barley during the entire period.

The pollen diagram for the Haraldstadmyr bog in the Sarpsborg area (Fig. 8c) depicts a slight decline in the sum fractions of anthropochores and apophytes coinciding with an increase in pollen from trees, starting just before 500 CE, followed by a slight and steady increase in the 6th century. From 500-600 CE, the percentages of anthropochores and apophytes remain more or less the same. The pollen for the individual cereals are sparse between 500-600 CE, including a total absence of *Triticum* (wheat) which, however, is not exclusive for this period. Small amounts of *Secale* (rye), *Hordeum* (barley), and *Avena* (oats) remain present. A decrease in charcoal percentages occurs slightly before 550 CE. Overall, fewer changes in pollen occur between 500-600 CE when compared to the Fron and Høgsfjorden areas.

(a)

Total no. pollen

Charcoal
Sordaria
Secale (rye)
Avena (oats)
Triticum (wheat)
Hordeum (barley)

Anthropochores
Apophytes

Trees

Cal. year CE

Depth (cm)

(b)
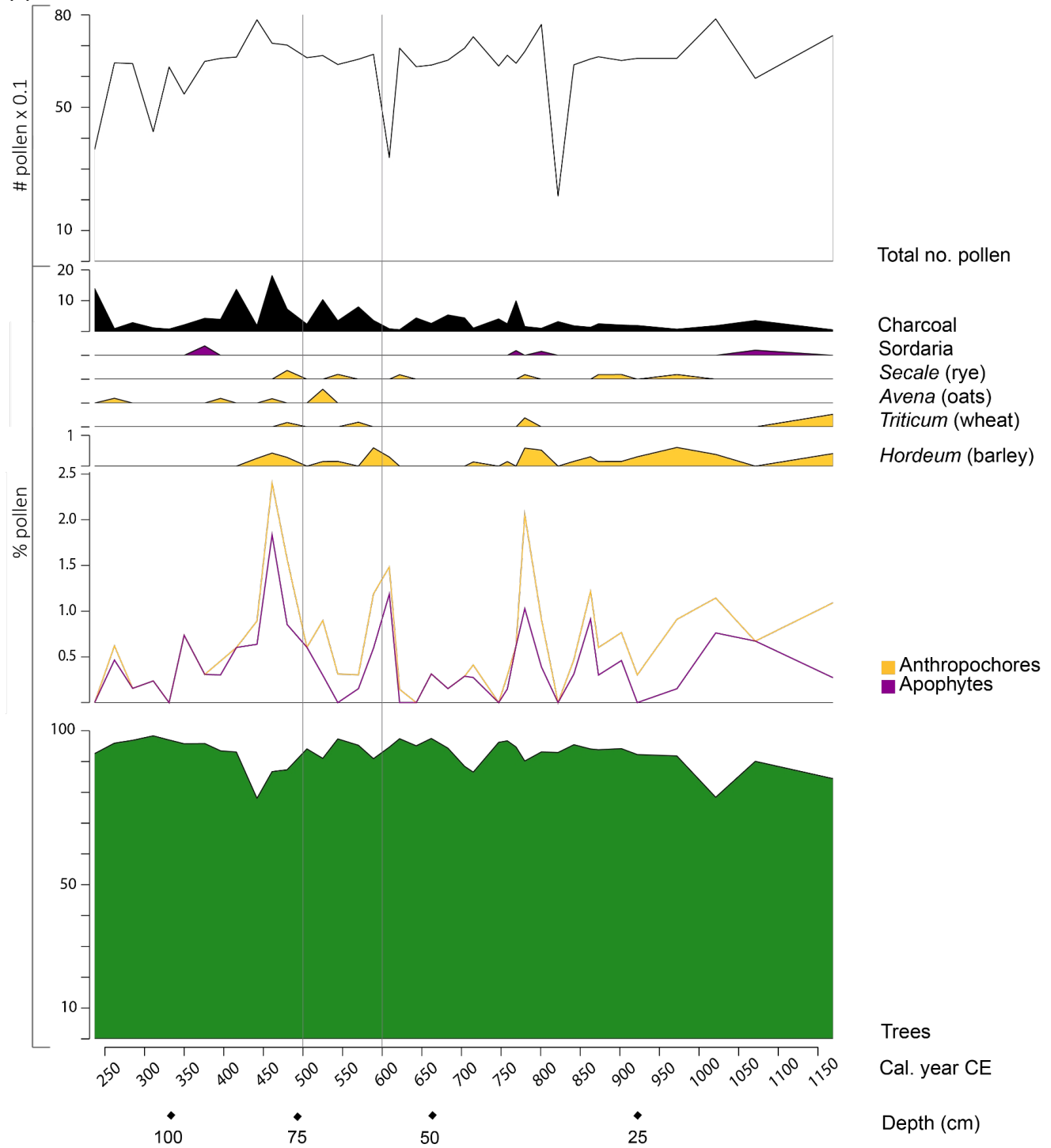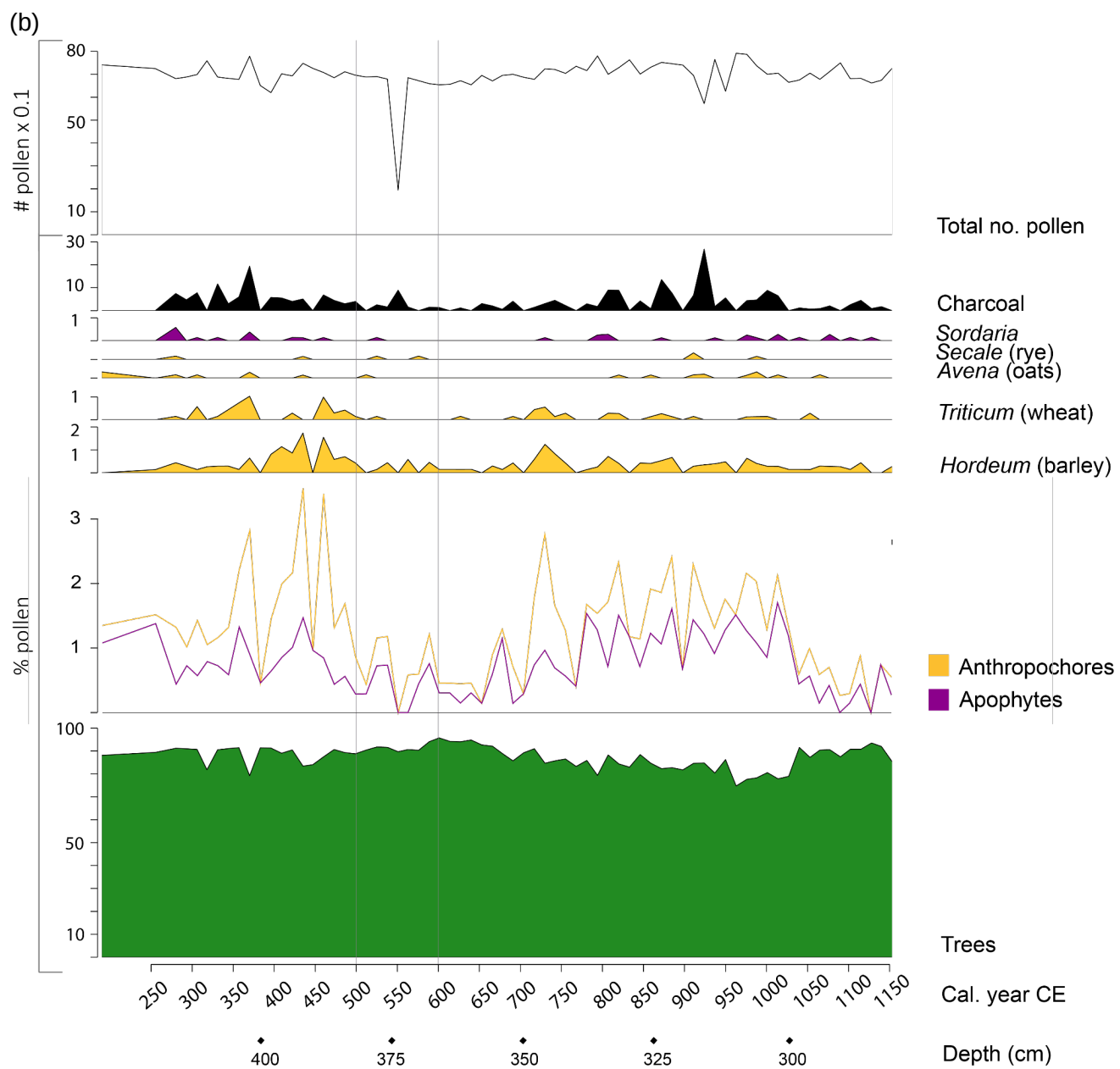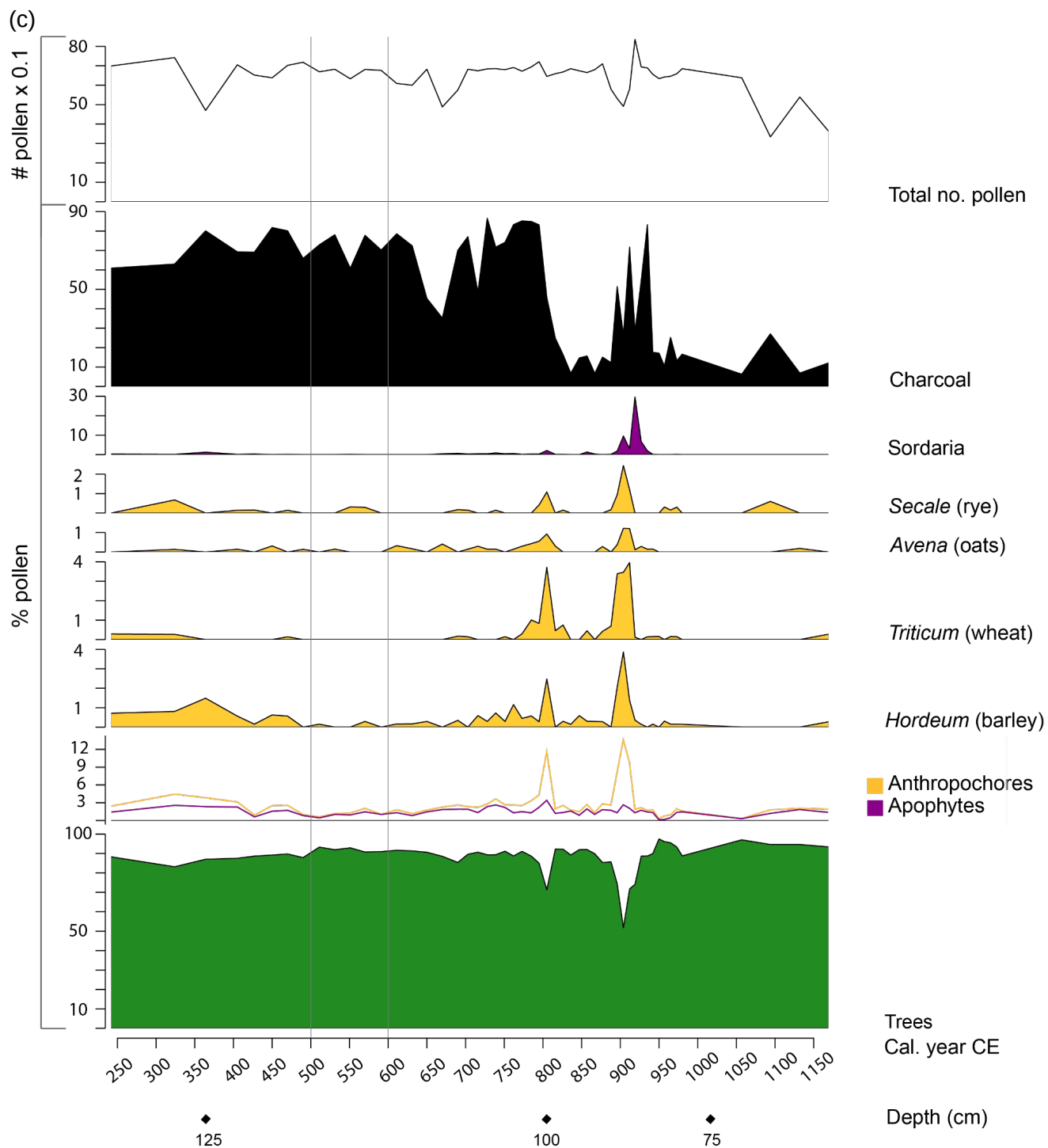
Figure 8. Pollen diagrams for a) Ulberg (Fron area), b) Åsheim (Høgsfjorden area), and c) Haraldstadmyr (Sarpsborg area).

4. Discussion

4.1 Volcanic climate model impact

The mean temperature response for both the short-term and the long-term after the 536/540 CE volcanic double event over Scandinavia is a significant cooling (Fig. 3a). In addition, we simulate a mean growing season 2m air temperature below 5 °C over parts of Scandinavia, which also includes
490   Fron. This could have implications for agriculture, as it is likely that the accumulated temperature sum fails to reach the GDD requirements for all cereal species. For precipitation, the ensemble mean indicates a drying over the entirety of Scandinavia for the 536-560 CE period as well as for the two years after the eruptions (Fig. 3b), which could also have impacted crop production. This drying is not surprising, as in general volcanic induced cooling leads to reduced precipitation/evaporation, as
495   colder air can hold less humidity. This is also in line with the findings of Büntgen et al. (2011), who studied the climate variability of the past 2500 years in Europe. They found a reduction in summer temperature due to volcanic eruptions coincided with a drying in the sixth century.

Iles and Hegerl (2014) analysed different types of datasets for the most recent eruptions in the period ~1900-2000 CE and found a drying over Scandinavia in the CMIP5 models. In contrast,
500   reanalysis data from their study as well as data based on satellite and rain gauge observations revealed a drying over Southern Scandinavia and wetter conditions over Northern Scandinavia. Thus, contrasting results have been found on the precipitation response to volcanic eruptions over Scandinavia in previous studies. This is in line with the findings of Tejedor et al. (2021), who studied the global hydroclimate response to large tropical volcanic eruptions using a paleo assimilation
505   product (PHYDA), which uses proxy data in a climate model, as well as an ESM on its own. PHYDA reconstructs a weak signal in the 20 years after all the large (larger than Pinatubo) tropical eruptions in the last millennium. Here it seems the west of Scandinavia is getting slightly dryer, and the rest getting slightly wetter. The Old World Drought Atlas (Cook et al., 2015) shows a more pronounced pattern than PHYDA, with a drying over the southern half of Scandinavia and a wetting in the north,
510   just as the reanalysis and observational data from Iles and Hegerl (2014) suggested. The signal of the drying in Southern Scandinavia and the wetting in Northern Scandinavia, however, is still not very strong (±1.5 on the PDSI scale). This could be a result of the averaging over 13 eruptions (all of potentially different magnitudes, chemical compositions and timing during the year), as well as taking the 20-year post-eruption mean. The data from Tejedor et al. (2021) mentioned before represent the
515   soil moisture availability over summer (JJA), and are therefore hard to directly compare to the simulated precipitation response from our climate model simulations. However, together with the precipitation response signal from the studies of Cook et al, (2015) and Iles and Hegerl (2014), they illustrate that the hydroclimate, including precipitation, is hard to simulate or reconstruct, especially when going further back in time (before the last millennium). Comparing the SLP anomalies,
520   precipitation anomalies, and the wind direction reveals that the post-volcanic precipitation patterns are connected to the atmospheric circulation (Figs. 6, A3).

The atmospheric circulation response after volcanic eruptions for the growing season in Scandinavia has not been studied in detail before. It encompasses the spring to late summer months, and the
525   model simulations show a positive like NAO pattern similar to the NH winter response in the 1-1850

CE climatology (Fig. A4). After Pinatubo, a positive NAO was observed, which generally leads to warmer and wetter winters in Scandinavia (Robock, 2000). Climate model simulations from the CMIP3/CMIP4 models, however, do not seem to capture this signal (Stenchikov et al., 2002; Driscoll et al., 2012). Ludlow et al. (2013) found severely cold winters over Ireland after tropical eruptions, implying a NAO- pattern following these eruptions. The winter warming pattern continues to be debated, and may be confined to the first winter after tropical eruptions (Zambri et al, 2017). The summertime atmospheric circulation over the European sector has also been studied, revealing a correlation between SLP patterns and changes in North Atlantic storm tracks (Hurell et al., 2003; Folland et al., 2009). The summertime NAO is defined by Hurell et al. (2003) as a similar mode to the NAO, but with a more confined centre in the Arctic and a more northern high pressure centre over northwestern Europe, for July-August. Zambri et al. (2019) studied the atmospheric circulation patterns for the individual ensemble members of their CESM 40-member ensemble after the Laki eruption from 1783-1784, which started in June. They found the temperature response over the North Atlantic sector to be dependent on the atmospheric circulation response. With a Scandinavian blocking the temperature response is a warming over northwestern Europe and without a blocking they find a cooling over all of Europe and Greenland. This is in line with our findings, where the different circulation responses in the individual ensemble members give different temperature and precipitation anomaly patterns.

The SLP anomaly in Fig. 4 shows that the atmospheric circulation response over Scandinavia is significant for the ensemble mean growing season for the 25-year mean (536-560 CE), but not for the 2-year mean after the 536 CE and 540 CE eruptions. The different patterns in the precipitation and SLP anomalies are cancelled out in the ensemble mean for both the long-term and the short-term response, resulting in a weak mean volcanic signal. Even though the 536-560 CE mean gives a significant increase in SLP over Scandinavia (Fig. 4a), the individual runs highlight differences in the regional responses as possible model realisations.

In the 2-year mean as well as the 25-year mean growing season (AMJJAS) after the eruptions, the general pattern shows a shift towards higher pressure over Scandinavia, corresponding to a shift towards a NAO- pattern. Simultaneously, a significant drying occurs over Norway and Sweden, accompanied by a reduction in the southwesterly 10 m winds (not shown). However, not all the ensemble members simulate this pattern. For example, ensemble member #2 simulates a strong cooling in 537 CE, as well as an increased pressure over Greenland and a decreased pressure over the North Atlantic west of Portugal, corresponding to a shift towards a NAO+. This leads to a precipitation pattern with wetter conditions over Western Norway and Central Eastern Sweden. In 541 CE, member #2 simulates a significant decrease in pressure over central Europe, corresponding to a shift towards a North Atlantic Ridge pattern. This corresponds to dry conditions in Western Norway and wet conditions in Eastern Sweden. This combination of decreased pressure over Europe and a dipole in precipitation over Scandinavia is visible in other members as well (#1 and #12).

Rising water levels in Eastern Swedish lakes and bogs have been reported for our period of interest. In approximately the mid-1st millennium CE, villages in Eastern Central Sweden were abandoned and resettled at higher locations, possibly due to the higher groundwater table (Gräslund and Price,

2012). Another indicator of rising water levels is the fungus *Claviceps purpurea*, commonly known as ergot, which thrives in cool areas with poor drainage and damp conditions (Alm and Elvevåg, 2013). In Southwest Norway ergot has been discovered at the Forsand excavation site (Løken, 2020), thus
570 suggesting wet conditions during our study period. A simulation such as ensemble member #2, with wetter conditions for both Southwestern Norway and Central Eastern Sweden, might therefore be considered as one of the more realistic volcanic climate scenarios.

4.2 GDD model

The GDD requirement numbers in Table 2 are based on experimental studies with traditional cereals
575 in the early 20th century conducted by Foss (1926, 1927). A multitude of local variants existed up to the introduction of standardised farming techniques in the 20th century, and the exact requirements for prehistoric crops are not known. This causes some uncertainty regarding the impact of climate change on Iron Age (500 BCE-1000 CE) farming. The GDD models should therefore be understood as a likely scenario on how volcanic cooling events could have affected Iron Age farming, and as a
580 method for demonstrating differences and similarities for crop cultivation potential in the three areas.

According to Foss (1926), failing to meet the required temperature sum is by no means directly synonymous with crop failure, but would result in smaller yields and a higher frequency of unripened grains unsuitable for sowing. Traditional farmers are likely to have secured themselves by long-term storage, but would only be able to sustain themselves in this way for a limited amount of time.
585 Surplus exchange between neighbouring households and communities may therefore have been an important measure against unforeseen events, thus stimulating the development of specialised craft and stratified societies (Halstead, 1989; O'Shea and Halstead, 1989). However, multiple years with low temperatures and poor harvests, potentially impacting societies on large spatial scales, would nonetheless gradually cause a lack of available sowing grains, thus making it difficult to maintain
590 production. A prolonged volcanic cooling could therefore make changes in subsistence strategies necessary, including a shift towards the selection of more robust species, adaptation in husbandry, and reliance on wildlife (e.g. hunting, foraging). The extent to which this actually occurred in our study areas must be substantiated by paleo-botanical and archaeological records.

Another issue that should be considered for the GDD modelling is the effect the volcanic aerosols
595 have on vegetation by impacting the available sunlight. There are several historical accounts in which a prolonged dimming of the sun was described for 536, concentrated in the Mediterranean (Stothers, 1984; Rampino et al., 1988; Costick and Ludlow, 2015). Less sunlight reaching the surface impacts the cultivation of cereals in a negative way by reducing the primary production over several years after the eruptions (Helama et al., 2018). On the other hand, the light following a
600 volcanic eruption is more diffuse because of the scattering effect of the volcanic aerosols, which is known to have a positive impact on plant growth (Fan et al., 2021). However, the GDD model is a simplified model, and these factors are not included. Here we have focused on temperature, precipitation, altitude, latitude, and growing season length. Still, for this study the GDD model is the appropriate tool to use. If daily output data from the climate model had been available, our modelled
605 present-day temperature and GDD estimates would be influenced by the climate model biases and the limited spatial resolution. Therefore, carrying out a scenario with a prescribed volcanic cooling,

and using this with the GDD model as we have done here, was considered more appropriate.

4.3 Pollen record
The pollen record shows a general decrease and low abundance of anthropochores and apophytes, i.e. indicators for human activity, between 500 CE and 600 CE, contemporary with an increase in
610   tree pollen. These findings suggest a decrease in human activity during the 6th century. This decrease is, however, expressed distinctively and to various extents between the different study areas.

In the Fron area, the anthropochores and apophytes show a distinct decline during the 6th century. The individual cereal taxa, however, display inconsistent signals during this period. Pollen from
615   wheat and barley show a decline, whereas pollen from oats show an increase between 500-550 CE. The increase in trees in the Fron area during the 6th century cooling, in combination with the decline in anthropochores and apopythes, is however a strong indicator for crisis and abandonment. The cereals rye, oats, and wheat, as direct indicators of cultivation, show a decline for the Høgsfjorden area in the 6th century, indicating crisis and abandonment. This interpretation is
620   strengthened by the coinciding increase in forest. Barley, however, varies to a great extent during the 6th century, implicating a highly irregular cultivation of the cereal throughout this period. The pollen record from the Sarpsborg area overall displays few transitions, regardless of pollen type, suggesting relatively stable conditions throughout the entire 6th century. The anthropochores and apophytes are relatively scarce in this period, a situation that continues into the 8th century.

625   In addition to the volcanic double event, there was an outbreak of the Justinian Plague in 541 CE. This has been proposed to have led to a decline of up to half the population in the Mediterranean area (Wagner et al., 2014), and has been found to have impacted societies as far as Germany (Harbeck et al., 2013) or the UK (Keller et al., 2019). If this was the case in Norway, this would have shown up in the pollen. However, even though the plague has been assumed to have reached
630   Scandinavia, no DNA has been found on skeletal remains so far (Gundersen, 2019). In addition, a recent study contests the idea of a dramatic population decline during the 6th to 8th century and downplays the possible importance of the plague for the social developments of the time (Mordechai et al., 2019). We therefore argue that the decline in pollen during this time was not likely a direct effect of the Justinian Plague, but may have been related to volcanically induced cooling. More work
635   is merited on this question.

The above pollen analyses have to be interpreted with caution with regard to the calibrated ages used in this study. We have dated between five and nine C14 samples per peat sequence. The C14 ages have a standard deviation (1σ) varying from 28 to 40 years. In addition, the mean ages in the pollen diagrams are dependent on interpolations made in the age-depth model. The age model could
640   be improved by detecting absolute time markers such as tephra in the bog sediments, which could be part of future work. However, the relative chronology of the transitions in the pollen record with regard to the depth axes remains unaffected by these factors. Other limitations that need to be taken into account include the production, depositional, dispersal and preservation processes of the pollen, which can cause an over- or under-representation of pollen types (Lowe and Walker, 2015).

645 Various pollen record studies analysing sediment cores in Scandinavia are available covering this period (Høeg, 1996; Høeg, 1997; Wiekowska-Lüth et al., 2017). However, they often span the entire Holocene and are sampled at ~10 cm intervals, giving a temporal resolution of ~120 years. The resolution in the pollen analyses in this study is higher, with sampling intervals of 1-3 cm in the period ~250- 1150 CE, giving a temporal resolution of ~8-24 years. As a result, the more detailed
650 pollen diagrams allow for a more in-depth analysis of shorter time intervals, such as the mid-6th century time period.

4.4 Case study areas

The results for the three case study areas suggest different levels of agricultural vulnerability to a volcanic cooling event, with Fron being particularly vulnerable and Sarpsborg being seemingly
655 resilient towards colder climate conditions. Høgsfjorden is at risk of experiencing reduced harvests, and even crop failure for heat demanding species. Here, we attempt to connect the GDD modelling, pollen analysis and archaeological records to describe possible volcanic climate hazard scenarios for the different areas.

Fron area
660 Fron is considered a dry area, and is located further north (north of 60°N) than the other two study areas, resulting in a reduction of the GDD requirements. However, Fron is also associated with a significantly shorter growing season as well as higher altitude. In addition, the landscape is hilly and rugged, which restricts the amount and extension of possible farmlands (Puschmann, 2005).

Three Iron Age farmsteads have been excavated in Fron in 2011-2012 (Loktu & Gundersen, 2016;
665 Villumsen, 2016). Their farming strategy was built on a combination of barley cultivation and animal husbandry. All of the farmsteads were occupied during the 5th century and subsequently abandoned during the 6th century. It has been suggested that the abandonment of the three farmsteads reflects a general decline in settlement and agriculture in Fron, as similar patterns have been documented on other agricultural sites in the area as well (Gundersen, 2016).
670
The pollen record from Fron shows a decrease in anthropochores and apophytes and an increase in trees in the mid-6th century, possibly confirming a short period of abandonment. Some crops, however, such as wheat and barley, sporadically continue to appear in the second half of the 6th century, followed by indications of a temporary halt in farming activity in the 7th century.

675 In addition, the farms were situated in areas exposed to floods and landslides, something that seems to have occurred more frequently around the mid-first millennium (Nesje et al., 2016). Around the late 6th or early 7th century, a major flood event buried one of the farmsteads under colluvial sediments, but the archaeological evidence shows that the site was abandoned prior to the flood (Villumsen, 2016). The exact time and character of the site abandonments are somewhat unclear,
680 but seem to have been planned and in response to environmental changes (Gundersen, 2021). The pollen record from nearby Ulberg (Section 4.3) also testifies to a decline and possible halt in crop cultivation around this time. The combined climate model and GDD simulations clearly suggest that the volcanic cooling event could have critically affected local agriculture in Fron, which may have

been further disrupted by an increase in flooding rates. However, the lack of widespread settlement
685   excavations in this area makes the scope and consequences of settlement abandonment unclear.

Høgsfjorden area
Høgsfjorden has similar temperature conditions as in the Oslofjord area in 1961-1990 (Fig. 7), but
also considerably higher precipitation levels (Table 2, Fig. 1b). The large amount of rainfall during
the growing season makes it necessary for higher temperatures for the cereals to mature, meaning
690   that the GDD requirements for cereal cultivation are higher than in the Sarpsborg area. The low
temperature margins for cultivation makes the Høgsfjorden area susceptible to climate anomalies,
which are a more regular feature in the western than the eastern part of Norway.

Large scale excavations have been conducted in the Høgsfjorden area, including a village complex
that was continuously occupied from the Bronze Age and up to the 6th century. The site is one of
695   very few settlements of this kind documented in Norway, and consisted in the 5th century of
approximately 20 farms (Løken, 2020). However, the 5th century village is also characterised by
increasing farming difficulties. Soil exhaustion due to intensive cattle grazing made crop cultivation
difficult, leading the farmers to turn to oat cultivation instead of barley and wheat. Oat is a thrifty
species and able to grow in poor and less nutritious soils, but is also associated with poor baking
700   qualities and low social status (Bjørnstad, 2012). In addition, it requires a high number of GDD to
mature (Table 2). Thus, what may have been a successful adaptation strategy in the 5th century
may have increased their vulnerability to the upcoming 6th century cold period. The GDD model for
this area suggests that a volcanic cooling event may have negatively affected oat harvests, and
potentially caused outright failure. The pollen data confirms this finding, showing a sharp decline in
705   both anthropochores and apophytes in the 6th century cold period, marked by the disappearance of
oats, wheat, rye and fungi from *Sordaria.*

The archaeological data also include finds of unmatured oat grains and examples of the fungus
Claviceps purpurea, commonly known as ergot (Løken, 2020). Ergot thrives in a cold and wet
climate and infects all sorts of grasses, including grains. It is also highly infectious and the cause for
710   numerous incidents of epidemic ergotism in historical times (Bondeson and Bondesson, 2014).
Thus, the archaeological evidence points in the direction of severe social impact from the cooling
event, which may have contributed to the final abandonment of the village around 600 CE. However,
it should be stressed that continuous settlement occupation has been documented at nearby
Forsandneset (Dahl, 2017), and that the abandonment of the village complex is not necessarily
715   representative of the whole Høgsfjorden area. A recent study of plant macrofossils and pollen data
from Rogaland county suggests that rye may have become important during the 6th and 7th
centuries due to colder climates (Westling and Jensen, 2020). Particularly important in this respect is
the site of Hove-Sørbø, which was contemporaneous with Forsand, but able to maintain settlement
and farming during and after the 6th century. Westling et al. (2022) argue that differences in soil
720   qualities and subsistence strategies were decisive for the profoundly different outcomes at the two
sites, thus demonstrating the importance of incorporating both human and environmental factors
when assessing social vulnerability to changing climates.

Sarpsborg area

The Sarpsborg area is characterised by relatively high temperatures, a long growing season, and low precipitation (Figs. 1b-c and Table 2). These factors, combined with the presence of extensive and fertile agricultural lands (Puschmann, 2005), provide excellent conditions for local agriculture, as well as high resilience against cold summers. The stable conditions for cultivation are reflected in the pollen data from Haraldstadmyr, as relatively few drastic transitions take place in the pollen record from 250 CE to 650 CE.

The area surrounding the Haraldstadmyr bog is characterised by numerous archaeological sites, but only a few of them have been excavated. Important are the recent excavations of a burial site and settlement site at Bjørnstad, situated only 400 metres to the north of Haraldstadmyr (Bårdseth, 2007; Rødsrud, 2007). The settlement site includes a large three-aisled building from around 800 CE that may have included a hall. Another settlement has been excavated at a nearby site at Tune, of what had probably been a farm building from around 400-700 CE (Bårdseth, 2006). The settlement is situated close to a burial site, 600 metres east of Haraldstadmyr, which was excavated in several phases during the 1900s. Characteristic for the Bjørnstad-Tune sites in the Sarpsborg area is the high percentage of Viking Age burials, which is somewhat in contrast to the rest of former Østfold county (Rødsrud, 2007). There is nonetheless a suggestive lack of Migration Period (400-550 CE) and Merovingian Period (550-800 CE) burials at the Bjørnstad site, which might be indicative of some kind of societal disruption, but with unclear temporal relation to 6th century circumstances. The pollen data indicates a period of slightly reduced farming activities from the mid-5th century to the mid-7th century, namely in the cultivation of cereals. However, due to its early onset, it is uncertain whether this period of reduced farming activities is related to the 6th century circumstances under study.

4.5 Archaeological radiocarbon dates

Radiocarbon datasets are shaped by numerous source-critical issues due to sampling strategies, research priorities, and investigation bias. Settlement sites from the Late Iron Age (c. 550–1000 CE) are for instance underrepresented in the Norwegian archaeological record, thus affecting the number of available C14 dates from this period. The C14 data can therefore not be used as exact expressions for the range and density of past human activities, but they are a tool for identifying peaks and troughs in the archaeological record. Whether such anomalies are more representative of past research priorities or past settlement activities is a matter of interpretation. As we have excluded cooking pits and iron and charcoal production sites and instead focused on comparable C14 data from throughout the Iron Age (500 BCE-1000 CE) (Section 2.3.1), the diagram (Fig. 9b) must be carefully scrutinised against research historical biases and how they condition data representativeness (Loftsgarden and Solheim, in press).

4.6 Synthesis

In this section, we try to bring all the lines of evidence together to sketch a likely scenario of how the
760   volcanic induced cooling could have impacted the local climate and society in Scandinavia. The
challenge of this study is to bring together different types of data with different spatial and temporal
resolutions, each with their own uncertainties. To connect the coarse spatial resolution from the
climate model to the local pollen and archaeological data, we utilised the GDD model. This acts as a
connector, enabling us to use the high temporal resolution information the climate model provides,
765   without losing the spatial variability between landscapes from the different case study areas.

The relatively good conditions for agriculture in the Sarpsborg area, even with a volcanic cooling, is
in contrast to the conditions for Fron and Høgsfjorden, which are associated with a higher degree of
vulnerability. However, the factors contributing to disaster risk in the latter two areas are nonetheless
of a different nature. Because of the dry climate and hilly and rugged landscape, the farming
770   landscape in Fron can be understood as marginal compared to the Sarpsborg area. This comparison
is, to a certain degree, also valid when it comes to Høgsfjorden, where the mountainous fjord
landscapes restrain the farming landscape in similar ways to Fron, but nonetheless include good
climate conditions for farming (Table 4; Puschmann, 2005). The available farmlands in the
Høgsfjorden area are heavily cultivated and considered productive. Flooding remains a considerable
775   challenge for agriculture and settlement in the Gudbrandsdalen valley, while Høgsfjorden is prone to
rough weather and high precipitation levels. Thus, although farming in both Fron and Høgsfjorden
may be vulnerable to colder conditions, the circumstances are different. Consequently, the course of
events leading up to possible harvest failures in the two areas would probably not be identical, and
may even be perceived as unrelated by those affected by them. These factors add to the complexity
780   of the potential disaster impact, and how it is experienced in a prehistoric context.

This is also reflected in the pollen data. The apophytes and antropochores in the Fron and
Høgsfjorden areas show a clear decline after ~500 CE, coinciding with an increase of forest,
whereas this is less evident in the pollen diagram for the Sarpsborg area. Charcoal, however, shows
a slight increase in the Fron area between 500-550 CE, the same as for the Sarpsborg area, and a
785   decline for the Høgsfjorden area. In addition, the pollen record from the Sarpsborg area indicates
stable conditions during 500-600 CE, as opposed to turbulent conditions in the Fron and
Høgsfjorden areas. Pollen data from other studies indicated a reduction in agriculture in the mid
sixth-century in areas in Southern Norway, Sweden and Estonia (Pedersen and Widgren, 2011;
Tvauri, 2014; Bajard et al., 2022). However, this is very area-dependent. Other archaeological and
790   pollen evidence from southwestern Norway and Sweden shows that not all areas experienced a
decline in agriculture (Randheden, 2007; Pedersen and Windgren, 2011). Similarly, Oinonen et al.
(2020) found an increase in burials in southwestern Finland (indicating an increase in population),
where the population seemed to have versatile livelihoods and rich natural resources, making them
not solely reliant on agricultural practices. In contrast, cultures a few hundred kilometres to the north
795   mainly relied on fishing and sealing. In these areas large settlements were abandoned around 550
CE.

Table 4. Summary of the different case study sites.

Area	Landscape	GDD model after volcanic cooling	Pollen	Farm abandonment
Fron	Mountainous	Crops fail	Decline in grain species	Clear evidence
Høgsfjorden	Fjord	Some crops fail	Decline in some grain species	Clear evidence, end of Forsand complex (Løken, 2020)
Sarpsborg	Clay-rich terminal moraines	Only wheat might fail	No change in grain species	No clear evidence

For the Høgsfjorden area there is evidence of ergot, indicating wet conditions (Løken, 2020). In eastern Sweden, wet conditions during the period after the 536/540 CE eruptions have also been
800 indicated (Gräslund and Price, 2012). Therefore, climate model ensemble members that simulate wetter conditions rather than a drying together with a pronounced cooling over Scandinavia pique our interest (Figs. A1 and A2). In addition to the evidence for site abandonment from our study areas, archaeological evidence for site abandonment in other areas (Solberg, 2000; Löwenborg, 2012) has also been taken into account here. Tree-ring reconstructions from northern Scandinavia
805 (Grudd, 2008; Esper et al., 2012) indicate a cooling of up to 3.5 °C after the 536/540 CE eruptions, which corresponds to the maximum cooling in the model ensemble members (Fig. A1). In addition, frost rings have been found in northern Finland after the 536 CE eruption (Helama et al., 2019), indicating freezing conditions during the growing season. Figure 9 depicts the above discussed climate and GDD model results together with archaeological evidence and pollen data for a
810 temperature and precipitation regime that shows a strong cooling, but also wet conditions over Southern Norway and central Sweden. The chosen climate model run and post-volcanic year is based on the temperature and precipitation pattern together. This is by no means the only feasible scenario for how the climate evolved after the 536/540 CE volcanic double event, but is instead an attempt to visualise several lines of evidence from different types of data and methods together. In
815 particular, precipitation is highly spatially variable, which makes it hard to reconstruct and/or model (Iles and Hegerl, 2014; Cook et al., 2015; Tejedor et al., 2021). Thus, we place higher confidence in the evidence for cooling after the eruptions, and the consequences this could have on the cultivation of crops and society.

The overall pattern is one of regional diversity concerning agricultural vulnerability to a large-scale
820 cooling event, which is further conditioned by the spatiotemporal complexity associated with weather and climate change. The social consequences of the 536/540 CE volcanic events should therefore not be treated as uniformly affecting all parts of Scandinavia. Our results suggest that climate change affected parts of Southern Norway in diverse ways. Although testifying to considerable social and material change, the Scandinavian archaeological record from around the mid-1st millennium
825 CE is also associated with contrasting regional patterns.

In Denmark, many old settlements were abandoned and new ones established (Nielsen, 2005;

2006). At Funen, villages appear to have been reorganised sometime around 600 CE (Hansen, 2016). However, there is also considerable regional variation and little evidence for an overall societal decline. Farming seems to have been reorganised and intensified (Näsman, 2009). Some areas include pollen evidence for reforestation of farmlands between 600-1000 CE, whereas others testify to deforestation and an expansion of heaths and pastures (Odgaard & Nielsen, 2009). Nielsen (2005; 2006) states that the development both precedes and succeeds the 6th century, which indicates that the 536/540 CE events may have functioned as a catalyst, but was probably not the main cause.

In Sweden, large-scale reorganisation has been documented in the Uppland area of Middle Sweden in and around the 6th century CE, resulting in larger and clustered settlements (Göthberg, 2007; Göthberg & Sundkvist, 2017). This process is usually understood in light of the emerging Late Iron Age magnate complex at Gamla Uppsala (Ljungkvist & Frölund, 2015), but also as evidence for a social crisis (Gräslund and Price, 2012). Pedersen and Widgren (2011) highlight the ambiguous nature of the archaeological and pollen record and argue that the Iron Age societies were unevenly affected by processes, depending on their subsistence and land-use strategies. According to the two authors, areas experiencing major expansions of the farming landscapes in the preceding centuries appear to have been the most vulnerable to the climate downturn.

As stated by Oinonen et al. (2020) in their study of the Levänluhta people of western Finland, a society based more on outfield- and marine resources would be less affected by crop failure than agrarian-dependent communities. Similar patterns are present in the Norwegian archaeological record.

The Norwegian landscape is highly diverse with spatially restricted but often heavily cultivated agricultural areas, and abundant outfields often rich in wildlife and resources. The level of dependency on farming outputs must have differed considerably in prehistoric times, as well as the character of farming strategies. Forsand in the 6th century is usually understood in terms of social crisis because of failing harvests and overgrazing by livestock (Løken, 2020; Westling et al., 2022), while Myhre (2002) emphasised examples of continuous settlement occupation and expansion in parts of Eastern and Middle Norway. However, Stamnes' (2016) GDD-modelling of Northern Trøndelag suggests that Middle Norway may have been vulnerable to a climate cooling as well, thus adding to the overall complexity. The C14-record for South-eastern Norway (Fig. 9b) is indicative of an overall reduction in archaeological sites during the 6th and 7th centuries. A lacuna in archeological finds around this time was early recognised and much debated in Norwegian archaeology, and explanations have ranged from ideas of crisis to a reorganisation of society by new and powerful elites (Gundersen, 2019).

However, there is no real contradiction between the two narratives and a new pictures is gradually emerging that indicates great diversity in disaster impact and human responses throughout Scandinavia, depending on the character of subsistence strategies, and local and regional variations in landscapes and climates, but also possible secondary and additional factors such as pandemics, social unrest, warfare, competition over resources, and trade disruptions (Gundersen, 2021). Our study contributes in this direction by utilising a wide range of cross-disciplinary datasets and

865   exploring the many facets of volcanic climate change on both regional and local scales. By contextualising the results, we have provided a diverse picture of the possible consequences of the 536/540 event for farming societies. However, although the present study demonstrates the potential of combining climate and GDD modelling with paleo-botany and archaeology, more issues should be thoroughly explored in order to be able to better understand the role of climate variations for social

870   change, in particular those addressing subsistence strategies in a wider sense than just farming. Important is the level of dependency to farming, but also how environmental disruptions to the human sphere interact with ongoing social processes, causing possible secondary and long-term effects that are more difficult to directly relate to the climate factor. Thus, more in-depth and broader studies are necessary.
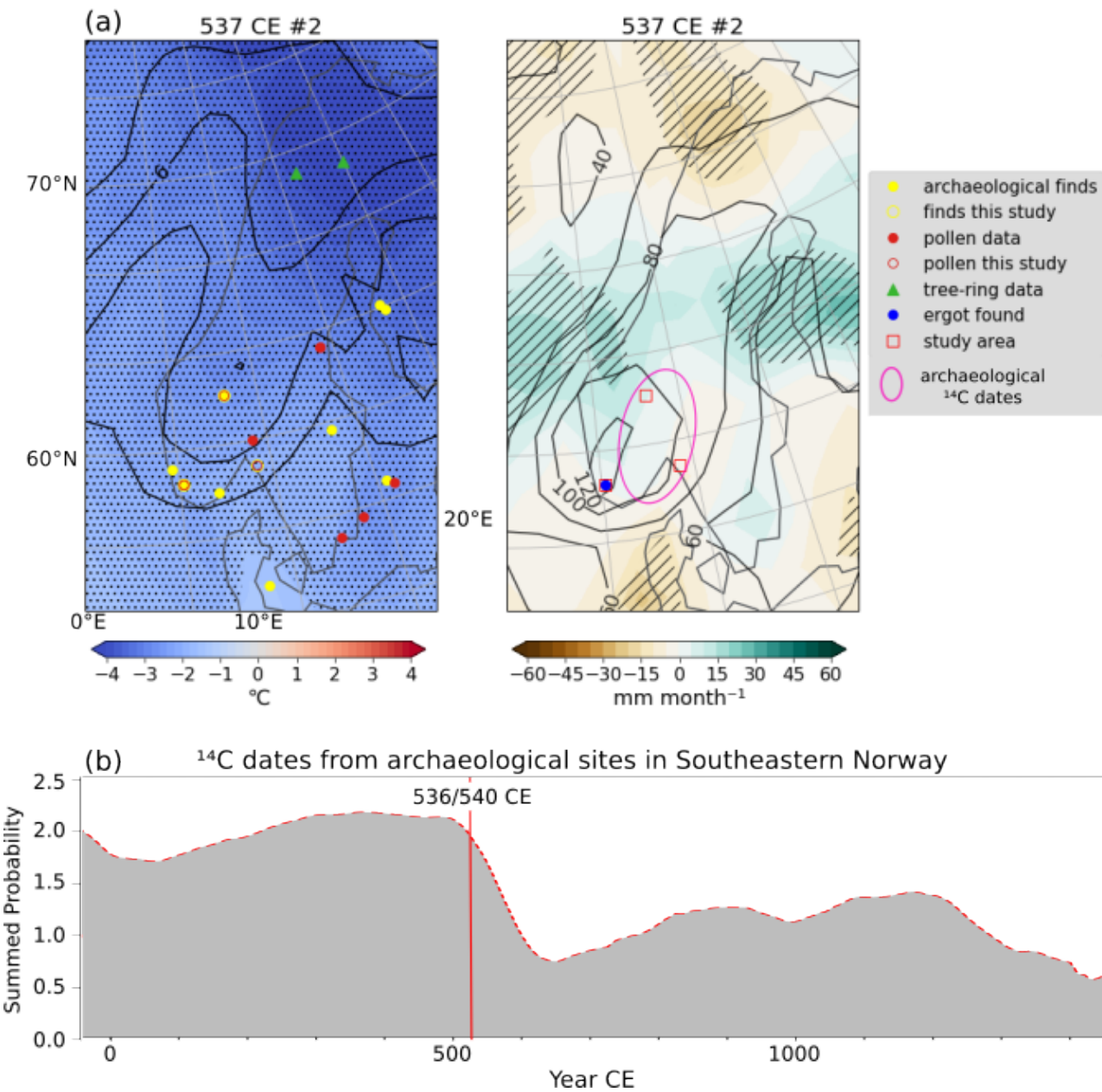
Figure 9. Synthesis figure. a) temperature and precipitation anomaly maps of Scandinavia from one realisation of the MPI-ESM model (ensemble member #2), with markers for archaeological, historical, and pollen proxy data supporting this model simulation. Pollen data showing reduction in agriculture in the mid-500s, archaeological finds indicating abandonment, and tree-ring reconstructions showing a 3.5 °C cooling in Northern Scandinavia 1-2 years after the 536 CE eruption. The data used for this figure are listed in Table A4. b) Summed probability distribution of 4012 ^{14}C dates (Loftsgarden and Solheim, in press) from archaeological sites in Southeastern Norway.

5. Conclusion

In this study, we have investigated the role of the 536/540 CE volcanic double event on the change in climate and society in Scandinavia, specifically in Southern Norway. Norway's landscape is diverse, with fjords, mountains, valleys, and coasts. This leads to an array of different climate and circulation regimes impacting cultivation practices. Three areas in Southern Norway were selected for a case study, based on different climates and landscapes, and the availability of excavation sites and high-resolution chronological pollen records.

The climate model ensemble mean projects a significant cooling over Scandinavia, and a drying for both the long-term 536-560 CE mean as well as for the first two growing seasons after the eruptions 536-537 CE and 540-541 CE. However, individual ensemble members exhibited regional differences for the temperature and precipitation anomalies, corresponding to the SLP anomaly patterns. Since the internal climate variability over Scandinavia is high and the model ensemble spread is large, the analyses focused on both the ensemble mean and on the individual members as possible volcanic climate impact realisations. For the period after the 536/540 CE volcanic double event, cold and wetter conditions have been indicated by both proxy climate and paleo-botanical evidence for Southwest Norway and central eastern Sweden, leading to the conclusion that realisations of the climate model ensemble that simulates colder and wetter conditions over these regions may be more realistic, although precipitation is highly variable in space and time.

The three selected case studies areas reveal in both the GDD model set-up as well as the pollen records that the areas on the west coast and the mountain areas of Southern Norway experienced a reduction in productivity, and even abandonment of sites in the mid-6th century, whereas the Oslofjord area in southeastern Norway showed less indication of crisis during that time. However, the effect on agriculture and society is a complicated picture and the overall impression is one of regionality and varying levels of disaster impact on Iron Age societies. Thus, neither in climatic nor societal terms, should the 6th century volcanically induced cooling be treated as uniform in its impacts throughout Scandinavia. On the contrary, it seems likely that it may have had different consequences throughout the peninsula, with considerable regional diversity in human responses to this unique volcanic climate hazard event.

Code and data availability
Primary data and scripts used in the analyses and other supplementary information that may be useful in reproducing the author's work are archived and can be obtained by request. Model data are now stored in the NIRD research data archive (https://doi.org/10.11582/2022.00029; Lorenz, 2022).

915 The PMIP4 past2k simulations contribute to CMIP6 and can be retrieved via the Earth System Grid
Federation network (e.g., https://esgf-475data.dkrz.de/search/cmip6-dkrz/). The GDD model is
based on meteorological data from MET Norway, available at seklima.met.no (last visited 25-07-
2022). Numerous Norwegian archaeological collections as well as almost all surveyed
archaeological sites, are digitised and available online (see unimus.no and Askeladden.ra.no).

Author contributions

920 EvD, IG, and KK conceived the original idea. EvD led the discussion and writing of the article. EvD
carried out the climate model runs, processed the data, performed the analysis, and designed the
figures for the model and synthesis parts. KK, CT, JJ contributed to the interpretation of the climate
model results. IG carried out the GDD model calculations and designed the GDD figures. FI and HH
cored the bogs. HH carried out the pollen sampling, analysis, counting and 14C sampling. AdB
925 analysed and designed the figures for the pollen data and constructed the age depth models. FI, IG,
and KL created the overview map and analysed the archeological sites. KK supervised the research
project. All authors discussed the results and helped write the manuscript.

Competing interests. The authors declare they have no competing interest.

Acknowledgements

930 This work is funded by the Norwegian Research Council (NRC)/University of Oslo Toppforsk project
'VIKINGS' with the grant number 275191. Computations, analysis and climate model data storage
were performed on the computer of the Deutsches Klima Rechenzentrum (DKRZ), and on Sigma2
the National Infrastructure for High Performance Computing and Data Storage in Norway. CT
acknowledges support for this research by the Deutsche Forschungsgemeinschaft Research Unit
935 VolImpact (FOR2820,398006378) within the project VolClim (TI 344/2-1). This work also benefited
from participation by some authors in the Past Global Changes Volcanic Impacts on Climate and
Society working group. We would like to thank Eirik Ballo and Anneke ter Schure for their help with
plotting the pollen diagrams and the discussion of the age models. Thanks to Robert David for
checking the English grammar and spelling. Finally, we would like to thank the reviewers and the
940 editor Francis Ludlow for their critical and helpful editorial comments.

References

Alm, T., & Elhevåg, B. 2013. Ergotism in Norway. Part 1: The symptoms and their interpretation from
the late Iron Age to the seventeenth century. History of Psychiatry, 24(1), 15-33.
doi:10.1177/0957154X11433960

945 Andersson, T. 2009: Altgermanische Ethnika, Namn och Bygd, 97:5–39.

Axboe, M., 1999. The year 536 and the Scandinavian gold hoards. Medieval Archaeology, 43.

Axboe, M., Capelle, T. and Fischer, C., 2005. Guld og guder. Ragnarok. Odins verden, pp.41-56.

Baillie, M.G., 1994. Dendrochronology raises questions about the nature of the AD 536 dust-veil

event. The Holocene, 4(2), pp.212-217.

950   Baillie, M.G., 2008. Proposed re-dating of the European ice core chronology by seven years prior to the 7th century AD. Geophysical Research Letters, 35(15).

Bajard, M., Ballo, E., Høeg, H.I., Bakke, J., Støren, E., Loftsgarden, K., Iversen, F., Hagopian, W., Jahren, A.H., Svensen, H.H. and Krüger, K., 2022. Climate adaptation of pre-Viking societies. Quaternary Science Reviews, 278, p.107374.

955   Berglund, B.E., Birks, H.J.B., Ralska-Jasiewiczowa, M. and Wright, H.E., 1996. Palaeoecological events during the last 15 000 years. Regional Syntheses of Palaeoecological Studies of Lakes and Mires in Europe. Whiley (Chichester).

Berglund, B.E., 2003. Human impact and climate changes—synchronous events and a causal link?. Quaternary International, 105(1), pp.7-12.

960   Bjørnstad, Å. 2012. Vårt daglege brød : kornets kulturhistorie (2. utg. ed.). Oslo: Vidarforlaget.

Blaauw, M. and J. A. Christen, 2011. Flexible paleoclimate age-depth models using an autoregressive gamma process. Bayesian Anal 6, 457–474.

Bondeson, L., & Bondesson, T. 2014. On the mystery cloud of AD 536, a crisis in dispute and epidemic ergotism: a linking hypothesis. Danish Journal of Archaeology, 3(1), 61-67.
965   doi:10.1080/21662282.2014.941176

de Bode, A. (2021) 'A pollen-based reconstruction of the paleoenvironment and cultural landscape in Southeastern Norway from the Iron Age to the Middle Ages'. Available at: https://hdl.handle.net/1887/3209493.

Briffa, K.R., Jones, P.D., Schweingruber, F.H. and Osborn, T.J., 1998. Influence of volcanic
970   eruptions on Northern Hemisphere summer temperature over the past 600 years. Nature, 393(6684), pp.450-455.

Brink, S., 2008. Law and society. The Viking World. London: Routledge, pp.23-31.

Brink, S. 2008a: People and land in early Scandinavia. In: P. Geary, P. Urbańczyk and I. H. Garipzanov (eds.): Franks, Northmen, and Slavs: Identities and State Formation in Early Medieval
975   Europe, Cursor Mundi, 5: 87–112. Brepols, Turnhout.

Büntgen, U., Tegel, W., Nicolussi, K., McCormick, M., Frank, D., Trouet, V., Kaplan, J.O., Herzig, F., Heussner, K.U., Wanner, H. and Luterbacher, J., 2011. 2500 years of European climate variability and human susceptibility. science, 331(6017), pp.578-582.

Büntgen, U., Myglan, V.S., Ljungqvist, F.C., McCormick, M., Di Cosmo, N., Sigl, M., Jungclaus, J.,
980   Wagner, S., Krusic, P.J., Esper, J. and Kaplan, J.O., 2016. Cooling and societal change during the

Late Antique Little Ice Age from 536 to around 660 AD. Nature geoscience, 9(3), pp.231-236.

Bårdseth, G. A. 2006. Huset på Store Tune - og nokre betraktningar om førhistoriske hus i Østfold. In H. Glørstad, B. Skar, & D. Skre (Eds.), Historien i forhistorien. Festskrift til Einar Østmo på 60-årsdagen (pp. 273-280). Oslo: Kulturhistorisk museum, Universitetet i Oslo.

985   Bårdseth, G. A., Sageider, B. M., & Sandvik, P. U. 2007. Busetjingsspor og mogleg hall frå yngre jarnalder på Bjørnstad søndre (lokalitet 11). In G. A. Bårdseth (Ed.), Hus, gard og graver langs E6 i Sarpsborg kommune. E6-prosjektet Østfold. Band 2 (pp. 71-90). Oslo: Kulturhistorisk museum, Fornminneseksjonen.

Bårdseth, G. A. 2008. Kulturhistorisk syntese. In G. A. Bårdseth (ed.), Evaluering - resultat. E6-
990   prosjektet Østfold. Band 5 (pp.79-104). Oslo: Kulturhistorisk museum, Fornminneseksjonen.

Carter, T., R. (1998). Changes in the thermal growing season in Nordic countries during the past century and prospects for the future. Agricultural and Food Science, 7(2), 161-179. doi:10.23986/afsci.72857

Cassou, C., 2008. Intraseasonal interaction between the Madden–Julian oscillation and the North
995   Atlantic Oscillation. Nature, 455(7212), pp.523-527.

Cook, E.R., Seager, R., Kushnir, Y., Briffa, K.R., Büntgen, U., Frank, D., Krusic, P.J., Tegel, W., van der Schrier, G., Andreu-Hayles, L. and Baillie, M., 2015. Old World megadroughts and pluvials during the Common Era. Science advances, 1(10), p.e1500561.

Crema, E.R., Bevan, A. 2020. Inference from large sets of radiocarbon dates: software and methods.
1000   Radiocarbon 63(1): 23–39. https://doi.org/10.1017/RDC.2020.95

Dahl, B., Husvegg, J. R., & Åhrberg, E. S. 2017. Arkeologisk og botanisk undersøkelse av hus i Bergevik. Berge gnr. 37 bnr. 1, Forsand kommune, Rogaland. Oppdragsrapport. Unpublished excavation report. Arkeologisk museum, Universitetet i Stavanger.

Damlien, H., Berg-Hanse, I. M., Melheim, L., Mjærum, A., Persson, P., Schülke, A., & Solheim, S.
1005   2021. Steinalderen i Sørøst-Norge. Faglig program for steinalderundersøkelser ved Kulturhistorisk museum. Oslo: Cappelen Damm akademisk NOASP.

Degroot, D., Anchukaitis, K., Bauch, M., Burnham, J., Carnegy, F., Cui, J., de Luna, K., Guzowski, P., Hambrecht, G., Huhtamaa, H. and Izdebski, A., 2021. Towards a rigorous understanding of societal responses to climate change. Nature, 591(7851), pp.539-550.

1010   Di Cosmo, N., Oppenheimer, C., & Büntgen, U. (2017). Interplay of environmental and socio-political factors in the downfall of the Eastern Türk Empire in 630 CE. Climatic change, 145(3), 383-395.

van Dijk, E., Jungclaus, J., Lorenz, S., Timmreck, C. and Krüger, K., 2021. Was there a volcanic

induced long lasting cooling over the Northern Hemisphere in the mid 6th–7th century?. Climate of the Past Discussions, pp.1-33.

1015 Driscoll, S., Bozzo, A., Gray, L.J., Robock, A. and Stenchikov, G., 2012. Coupled Model Intercomparison Project 5 (CMIP5) simulations of climate following volcanic eruptions. Journal of Geophysical Research: Atmospheres, 117(D17).

Esper, J., Büntgen, U., Timonen, M. and Frank, D.C., 2012. Variability and extremes of northern Scandinavian summer temperatures over the past two millennia. Global and Planetary Change, 88,
1020 pp.1-9.

Fan, Y., Tjiputra, J., Muri, H., Lombardozzi, D., Park, C.E., Wu, S. and Keith, D., 2021. Solar geoengineering can alleviate climate change pressures on crop yields. Nature Food, 2(5), pp.373-381.

Folland, C.K., Knight, J., Linderholm, H.W., Fereday, D., Ineson, S. and Hurrell, J.W., 2009. The
1025 summer North Atlantic Oscillation: past, present, and future. Journal of Climate, 22(5), pp.1082-1103.

Foss, H. (1926). Beretning fra Statens forsøksstasjon for fjellbygdene 1925. Ottende arbeidsår. Forsøk med rug og hvete i fjellbygdene. Oslo: Grøndahl & Søns Boktrykkeri.

Foss, H. (1927). Kornavl i fjellbygder. Oslo: Cappelen.

1030 Frøseth, R. B. (2004). Korn. In G. L. Serikstad (Ed.), Økologisk handbok. Matvekster (pp. 167-187). Oslo: GAN Forlag.

Goring, S., Dawson, A., Simpson, G. L., Ram, K., Graham, R. W., Grimm, E. C., and J. W. Williams, 2015. neotoma: A Programmatic Interface to the Neotoma Paleoecological Database. Open Quaternary 1(1), Art. 2. DOI: 10.5334/oq.ab

1035 Gräslund, B. and Price, N., 2012. Twilight of the gods? The 'dust veil event'of AD 536 in critical perspective. Antiquity, 86(332), pp.428-443.

Grudd, H., 2008. Torneträsk tree-ring width and density AD 500–2004: a test of climatic sensitivity and a new 1500-year reconstruction of north Fennoscandian summers. Climate dynamics, 31(7), pp.843-857.

1040 Gundersen, I. M. 2016. Jordbruksbosetninger i dalbunnen. Fellestrekk. In I. M. Gundersen (Ed.), Gård og utmark i Gudbrandsdalen. Arkeologiske undersøkelser i Fron 2011-2012 (pp. 121-130). Kristiansand: Portal forlag.

Gundersen, I. M. 2019. The Fimbulwinter theory and the 6th century crisis in the light of Norwegian archaeology: Towards a human-environmental approach. Primitive tider, 21, pp.101-119.

1045   Gundersen, I. M., Rødsrud, C. L., & Post-Melbye, J. R. 2020: Kokegroper som massemateriale. Regional variasjon i en kulturhistorisk brytningstid. In C. Rødsrud Løchsen & A. Mjærum (Eds.), Ingen vei utenom. Arkeologiske utgravninger i knyttet til etablering av ny riksveg 3 og 25 i Løten og Elverum kommuner, Innlandet (pp. 187-199). Oslo: Cappelen Damm Akademisk forlag.

Gundersen, I. M. 2021. Iron Age Vulnerability. The Fimbulwinter hypothesis and the archaeology of
1050   the inlands of eastern Norway. (PhD Monograph). University of Oslo, Oslo.

Göthberg, H. 2007. Mer än bara hus och gårdar. In H. Göthberg (Ed.), Hus och bebyggelse i Uppland. Delar av förhistorisk sammanhang (Vol. 3). Uppsala: Riksantikvarieämbetet.

Göthberg, H., & Sundkvist, A. 2017. Järnalderns gårdsmiljöer - tradition och förandring under tusen år. In L. B. Jörpeland, H. Göthberg, A. Seiler, & J. Wikborg (Eds.), at Uppsalum - människor och
1055   landskapande. Utbyggnad av Ostkustbanan genom Gamla Uppsala (pp. 21-46). Stockholm: Arkeologerna, Statens historiska museer.

Harbeck, M., Seifert, L., Hänsch, S., Wagner, D. M., Birdsell, D., Parise, K. L., ... & Scholz, H. C. (2013). Yersinia pestis DNA from skeletal remains from the 6th century AD reveals insights into Justinianic Plague. PLoS pathogens, 9(5), e1003349.

1060   Hatlestad, K., Wehlin, J., and Lindholm, K.-J. (2021). Coping with Risk. A Deep-Time Perspective on Societal Responses to Ecological Uncertainty in the River Dalälven Catchment Area in Sweden. *Land*, 10(8), 883.

Halstead, P. 1989. The economy has a normal surplus: economic stability and social change among early farming communities of Thessaly, Greece. In J. O'Shea & P. Halstead (Eds.), Bad Year
1065   Economics: Cultural Responses to Risk and Uncertainty (pp. 68-80). Cambridge: Cambridge University Press.

Hansen, J.(2016. Landsbydannelse og bebyggelsesstruktur i 1. årtusinde. En præsentation af et bebyggelseshistorisk regionalstudie. In K. Cassel (Ed.), Socioekonomisk mångfald. Ritualer och urbanitet: Rapport från projektseminarium för Ostkustbanan (OKB) genom Gamla Uppsala (pp. 11-
1070   26). Stockholm & Uppsala: Statens Historiska Museer, Arkeologerna.

Hanssen-Bauer, I., Førland, E. J., Haddeland, I., Hisdal, H., Mayer, S., Nesje, A., . . . Ådlandsvik, B. (2017). Climate in Norway 2100 – a knowledge base for climate adaptation(Vol. 1/2017).

Hegerl, G.C., Crowley, T.J., Hyde, W.T. and Frame, D.J., 2006. Climate sensitivity constrained by
1075   temperature reconstructions over the past seven centuries. Nature, 440(7087), pp.1029-1032.

Helama, S., Jones, P.D. and Briffa, K.R., 2017. Limited late antique cooling. Nature Geoscience, 10(4), pp.242-243.

Helama, S., Arppe, L., Uusitalo, J., Holopainen, J., Makela, H. M., Makinen, H., . . . Oinonen, M. (2018). Volcanic dust veils from sixth century tree-ring isotopes linked to reduced irradiance, primary
1080 production and human health. Sci Rep, 8(1), 1-12. doi:10.1038/s41598-018-19760-w

Helama, S., Saranpää, P., Pearson, C.L., Arppe, L., Holopainen, J., Mäkinen, H., Mielikäinen, K., Nöjd, P., Sutinen, R., Taavitsainen, J.P. and Timonen, M., 2019. Frost rings in 1627 BC and AD 536 in subfossil pinewood from Finnish Lapland. Quaternary Science Reviews, 204, pp.208-215.

Hkr = Snorri Sturluson Heimskringla I-II: Old Norse version: Islenzk fornrit, 1941 (1979). Bjarni
1085 Agalbjarnarsson (ed.). Reykjavík. Norwegian translation: Heimskringla, utgave Kongesagaer/ Snorre Sturluson (Translated by Anne Holtsmark and Didrik Arup Seip (1979), Norges kongesagaer, 1–2. Oslo.

Høeg, H.I., 1996. Varia 39 Pollenanalytiske undersøkelser i" Østerdalsområdet" med hovedvekt på Rødsmoen, Åmot i Hedmark. Varia http://urn. nb. no/URN: NBN: no-42007.

1090 Høeg, H.I., 1997. Varia 46 Pollenanalytiske undersøkelser på Øvre Romerike, Ullensaker og Nannestad, Akershus kommune. Varia http://urn. nb. no/URN: NBN: no-42007.

Høeg, H. I. 1999. Pollenanalytiske undersøkelser i Rogaland og Ersdal i Vest-Agder. In L. Selsing & G. Lillehammer (Eds.), Museumslandskap. Artikkelsamling til Kerstin Griffin på 60-års-dagen (Vol. AmS-Rapport 12A, pp. 145-225). Stavanger: Arkeologisk museum.

1095 Hines, J. and IJssennagger, N. eds., 2017. Frisians and Their North Sea Neighbours: From the Fifth Century to the Viking Age. Boydell & Brewer.

Hurrell, J.W., 1995. Decadal trends in the North Atlantic Oscillation: Regional temperatures and precipitation. Science, 269(5224), pp.676-679.

Hurrell, J.W., Kushnir, Y., Ottersen, G. and Visbeck, M., 2003. An overview of the North Atlantic
1100 oscillation. Geophysical Monograph-American Geophysical Union, 134, pp.1-36.

Indrebø, G.L., 1932. Fylke og fylkesnamn.

Iversen, F. 2016. Estate division: Social cohesion in the aftermath of AD 536-7. In F. Iversen & H. Petersson (Eds.), The Agrarian Life of the North 2000 BC AD 1000: Studies in Rural Settlement and Farming in Norway (pp. 41-76). Kristiansand: Portal Academic.

1105 Iversen, F., 2019. Between Tribe and Kingdom: People, land, and law in Scandia AD 500-1350. Rulership in 1st to 14th century Scandinavia royal graves and sites at Avaldsnes and beyond, Dagfinn Skre (ed.), De Gruter, Berlin, pp.245-304.

Iversen, F. and Brendalsmo, J., 2020. Den tidlige kirkeorganisasjonen i Eidsivatingslagen. Collegium Medievale, 33, pp.113-162.

1110 Iversen, F. (2021). The Four Petty Kingdoms of Upplǫnd: Equestrian Graves and the Political Integration of the Norwegian Highlands in Late Viking Age Norway. Viking, 84(1), 13-42. doi:10.5617/viking.9046

Juggins, S., 2020. rioja: Analysis of Quaternary Science Data. R package version 0.9-26, https://cran.r-project.org/package=rioja.

1115 Jungclaus, J.H., Bard, E., Baroni, M., Braconnot, P., Cao, J., Chini, L.P., Egorova, T., Evans, M., González-Rouco, J.F., Goosse, H. and Hurtt, G.C., 2017. The PMIP4 contribution to CMIP6–Part 3: The last millennium, scientific objective, and experimental design for the PMIP4 past1000 simulations. Geoscientific Model Development, 10(11), pp.4005-4033.

Keller, M., Spyrou, M. A., Scheib, C. L., Neumann, G. U., Kröpelin, A., Haas-Gebhard, B., ... &
1120 Krause, J. (2019). Ancient Yersinia pestis genomes from across Western Europe reveal early diversification during the First Pandemic (541–750). Proceedings of the National Academy of Sciences, 116(25), 12363-12372.

Kostick, C., & Ludlow, F. (2015). The dating of volcanic events and their impact upon European society, 400–800 CE. *Post-Classical Archaeologies*, *5*, 7-30.

1125 Larsen, L.B., Vinther, B.M., Briffa, K.R., Melvin, T.M., Clausen, H.B., Jones, P.D., Siggaard-Andersen, M.L., Hammer, C.U., Eronen, M., Grudd, H. and Gunnarson, B.E., 2008. New ice core evidence for a volcanic cause of the AD 536 dust veil. Geophysical Research Letters, 35(4).

Little, L.K., 2006. Plague and the end of antiquity: the pandemic of 541-750. Cambridge University Press.

1130 Loftsgarden, K. 2020 Mass production and mountain marketplaces in Norway in the Viking and Middle Ages. Medieval Archaeology 64: 94–115.

Loftsgarden, K. and S. Solheim. In press. Uncovering population dynamics in Southeastearn Norway from 1300 BC to AD 800 using summed radiocarbon probability distributions. In: Ystgaard, I. and M.
1135 Ødegaard (Eds.), Complexity and dynamics: Settlement and landscape from the Iron Age and Medieval period in the Nordic Countries. Sidestone Press

Loktu, L., & Gundersen, I. M. 2016. Jernaldergårdene ved Breivegen. Kontinuitet og endring over 300 år. In I. M. Gundersen (Ed.), Gård og utmark i Gudbrandsdalen. Arkeologiske undersøkelser i Fron 2011-2012 (pp. 145-165). Kristiansand: Portal forlag.

1140 Lowe, J.J., Walker, M. and Walker, M.J.C., 2015. Geomorphological evidence. Reconstructing Quaternary Environments: New York, Routledge, pp.19-92.

Løken, T. 2020. Bronze Age and Early Iron Age house and settlement development at Forsandmoen, south-western Norway. Stavanger: Museum of Archaeology, University of Stavanger.

Löwenborg, D., 2012. An Iron Age shock doctrine: did the AD 536-7 event trigger large-scale social changes in the Mälaren valley area?. Journal of Archaeology and Ancient History (JAAH), (4).

Malone, K. 1962: Widsith. Rosenkilde and Bagger, Copenhagen.

Mauritsen, T., Bader, J., Becker, T., Behrens, J., Bittner, M., Brokopf, R., Brovkin, V., Claussen, M., Crueger, T., Esch, M. and Fast, I., 2019. Developments in the MPI-M Earth System Model version 1.2 (MPI-ESM1. 2) and its response to increasing CO2. Journal of Advances in Modeling Earth Systems, 11(4), pp.998-1038.

McCormick, M., Büntgen, U., Cane, M.A., Cook, E.R., Harper, K., Huybers, P., Litt, T., Manning, S.W., Mayewski, P.A., More, A.F. and Nicolussi, K., 2012. Climate change during and after the Roman Empire: reconstructing the past from scientific and historical evidence. Journal of Interdisciplinary History, 43(2), pp.169-220.

McIlveen, J. F. R. (1986). Basic meteorology : a physical outline. Wokingham & Berkshire: Van Nostrand Reinhold UK.

Michelangeli, P.A., Vautard, R. and Legras, B., 1995. Weather regimes: Recurrence and quasi stationarity. Journal of the atmospheric sciences, 52(8), pp.1237-1256.

Miller, G.H., Geirsdóttir, Á., Zhong, Y., Larsen, D.J., Otto-Bliesner, B.L., Holland, M.M., Bailey, D.A., Refsnider, K.A., Lehman, S.J., Southon, J.R. and Anderson, C., 2012. Abrupt onset of the Little Ice Age triggered by volcanism and sustained by sea-ice/ocean feedbacks. Geophysical Research Letters, 39(2).

Mordechai, L., Eisenberg, M., Newfield, T. P., Izdebski, A., Kay, J. E., & Poinar, H. (2019). The Justinianic Plague: an inconsequential pandemic?. Proceedings of the National Academy of Sciences, 116(51), 25546-25554.

Munch, P.A., 1849. Historisk-geographisk beskrivelse over kongeriget Norge (Noregsveldi) i middelalderen. Wilhelm Grams Forlag.

Myhre, B. 2002. Landbruk, landskap og samfunn 4000 f.Kr.-800 e.Kr. In B. Myhre & I. Øye (Eds.), Jorda blir levevei : 4000 f.Kr.-1350 e.Kr (pp. 11-213). Oslo: Samlaget.

Neidorf, L. 2013: The Dating of Widsith and the Study of Germanic Antiquity. Neophilologus, 97:165–83.

Nesje, A., Gundersen, I. M., & Cannell, R. 2016. Flommer og flomskred i Gudbrandsdalen i et værmessig og klimatisk perspektiv. In I. M. Gundersen (Ed.), Gård og utmark i Gudbrandsdalen. Arkeologiske undersøkelser i Fron 2011-2012 (pp. 80-93). Kristiansand: Portal forlag.

Nielsen, K. H. 2005. "... the sun was darkened by day and the moon by night ... there was distress

among men ..." - on social and political development in the 5th- to 7th-century southern Scandinavia. In H.-J. Häßler (Ed.), Neue Forschungsergebnisse zur nordwesteuropäischen Frühgeschichte unter besonderer Berücksichtigung der altsächsischen Kultur im heutigen Niedersachsen (pp. 247-285). Oldenburg: Isensee Verlag.

1180 Nielsen, K. H. 2006. Abundant Gold and Bad Harvests: Changes in Southern Scandinavian Society during the 5th to 7th Centuries. In M. Bertasius (Ed.), Transformatio mundi. The transition from the late migration period to the early Viking age in the east Baltic (pp. 41-50). Kaunas: Kaunas University of Technology, Department of Philosophy and Cultural Science.

Odgaard, B., & Nielsen, A. B. 2009. Udvikling i arealdækning i perioden 0-1850. Pollen og
1185 landskabshistorie. In B. Odgaard & J. R. Rømer (Eds.), Danske landbrukslandskaper gennem 2000 år. Fra digevoldinger til støtteordninger (pp. 41-58). Århus: Aarhus Universitetsforlag.

Oinonen, M., Alenius, T., Arppe, L., Bocherens, H., Etu-Sihvola, H., Helama, S., Huhtamaa, H., Lahtinen, M., Mannermaa, K., Onkamo, P. and Palo, J., 2020. Buried in water, burdened by nature— Resilience carried the Iron Age people through Fimbulvinter. PloS one, 15(4), p.e0231787.

1190 O'Shea, J. & Halstead, P. 1989. Conclusion: bad year economics. In J. O'Shea & P. Halstead (Eds.), Bad Year Economics: Cultural Responses to Risk and Uncertainty (pp. 123-126). Cambridge: Cambridge University Press.

Pedersen, E.A., Norseng, P.G. and Stylegar, F.A., 2003. Østfolds historie: Øst for Folden. Bind 1. Østfold fylkeskommune.

1195 Procopius. (1919 [~530-560]). History of the Wars, Volume III (H. B. Dewing, Trans.). In Loeb classical library: Harvard University Press.

Puschmann, O., 2005. Nasjonalt referansesystem for landskap. Beskrivelse av Norges 45 landskapsregioner. NIJOS rapport 10/2005, Ås.

Stothers, R. B., & Rampino, M. R. (1983). Volcanic eruptions in the Mediterranean before AD 630
1200 from written and archaeological sources. Journal of Geophysical Research: Solid Earth, 88(B8), 6357-6371.

Rampino, M.R., Self, S. and Stothers, R.B., 1988. Volcanic winters. Annual Review of Earth and Planetary Sciences, 16(1), pp.73-99.

Ranheden, H. (2007). Vegetationsförendringar. In E. Hjärthner-Holdar, H. Ranheden, & A. Seiler
1205 (Eds.), Land och samhälle i förändring. Uppländska bygder i ett långtidsperspektiv (Vol. vol. 4, pp. 17-118). Uppsala: Riksantikvarieämbetet, Upplandsmuseet, Societas Archaeologica Upsaliensis.

Reimer, P.J., Austin, W.E., Bard, E., Bayliss, A., Blackwell, P.G., Ramsey, C.B., Butzin, M., Cheng, H., Edwards, R.L., Friedrich, M. and Grootes, P.M., 2020. The IntCal20 Northern Hemisphere

radiocarbon age calibration curve (0–55 cal kBP). Radiocarbon, 62(4), pp.725-757.

1210 Robock, A. (2000). Volcanic eruptions and climate. *Reviews of geophysics*, *38*(2), 191-219.

Rosen, W., 2006. Justinian's flea: plague, empire and the birth of Europe. Random House.

Rødsrud Løchsen, C. 2007. Graver og bosetningsspor på Bjørnstad (lokalitet 44). In G. A. Bårdseth (Ed.), Hus, gard og graver langs E6 i Sarpsborg kommune. E6-prosjektet Østfold. Band 2 (pp. 91-183). Oslo: Kulturhistorisk museum, Fornminneseksjonen.

1215 ter Schure, A.T.M., Bajard, M., Loftsgarden, K., Høeg, H.I., Ballo, E., Bakke, J., Støren, E.W.N., Iversen, F., Kool, A., Brysting, A.K. and Krüger, K., 2021. Anthropogenic and environmental drivers of vegetation change in southeastern Norway during the Holocene. Quaternary Science Reviews, 270, p.107175.

Sigl, M., McConnell, J.R., Layman, L., Maselli, O., McGwire, K., Pasteris, D., Dahl-Jensen, D.,
1220 Steffensen, J.P., Vinther, B., Edwards, R. and Mulvaney, R., 2013. A new bipolar ice core record of volcanism from WAIS Divide and NEEM and implications for climate forcing of the last 2000 years. Journal of Geophysical Research: Atmospheres, 118(3), pp.1151-1169.

Sigl, M., Winstrup, M., McConnell, J.R., Welten, K.C., Plunkett, G., Ludlow, F., Büntgen, U., Caffee, M., Chellman, N., Dahl-Jensen, D. and Fischer, H., 2015. Timing and climate forcing of volcanic
1225 eruptions for the past 2,500 years. Nature, 523(7562), pp.543-549.

Skre, D., 2019. Rulership and Ruler's Sites in 1st–10th-century Scandinavia. Rulership in 1st to 14th century Scandinavia royal graves and sites at Avaldsnes and beyond, Dagfinn Skre (ed.), De Gruter, Berlin, pp.193-243.

Solberg, B. (2000). *Jernalderen i Norge: ca. 500 f. Kr.-1030 e. Kr*. Cappelen akademisk forlag.

1230 Solberg, B., 2006. Signs, symbols and mortuary rituals in the period 200-550/70 AD in Norway. UBAS Nordisk 3. Samfunn, symboler og identitet. Festskrift til Gro Mandt på 70-årsdagen.

Stamnes, A. A. (2016). Effect of temperature change on Iron Age cereal production and settlement patterns in Mid-Norway. In F. Iversen & H. Petersson (Eds.), The Agrarian Life of the North 2000 BC AD 1000 : Studies in Rural Settlement and Farming in Norway (pp. 27-40).
1235 Kristiansand: Portal Academic.

Stenchikov, G., Robock, A., Ramaswamy, V., Schwarzkopf, M.D., Hamilton, K. and Ramachandran, S., 2002. Arctic Oscillation response to the 1991 Mount Pinatubo eruption: Effects of volcanic aerosols and ozone depletion. Journal of Geophysical Research: Atmospheres, 107(D24), pp.ACL-28.

1240 Stothers, R.B., 1984. Mystery cloud of AD 536. Nature, 307(5949), pp.344-345.

Strand, E. (1984). Korn og korndyrking. Oslo: Landbruksforlaget.

Sturluson, S. (1963 [~1220-1230]). Kringla heimsins (S. Schjøtt, Trans.). In Kongesoger: Soga om Olav den heilage (Vol. 21). Oslo: Samlaget

TeBrake, W.H., 1978. Ecology and economy in early medieval Frisia. Viator, 9, pp.1-30.

1245   Tedesco, Paulina Souza. Joint modeling of low temperature and low wind speed events over Europe conditioned on winter weather regimes. Master thesis, University of Oslo, 2020.

Tejedor, E., Steiger, N.J., Smerdon, J.E., Serrano-Notivoli, R. and Vuille, M., 2021. Global hydroclimatic response to tropical volcanic eruptions over the last millennium. Proceedings of the National Academy of Sciences, 118(12).

1250   Toohey, M., Krüger, K., Sigl, M., Stordal, F. and Svensen, H., 2016. Climatic and societal impacts of a volcanic double event at the dawn of the Middle Ages. Climatic Change, 136(3), pp.401-412.

Toohey, M., & Sigl, M. (2017). Volcanic stratospheric sulfur injections and aerosol optical depth from 500 BCE to 1900 CE. Earth System Science Data, 9(2), 809-831.

Tvauri, A., 2014. The impact of the climate catastrophe of 536–537 AD in Estonia and neighbouring
1255   areas. Eesti Arheoloogia Ajakiri, 18(1), pp.30-56.

Van Loon, H., & Rogers, J. C. (1978). The seesaw in winter temperatures between Greenland and northern Europe. Part I: General description. Monthly Weather Review, 106(3), 296-310.

Vautard, R., 1990. Multiple weather regimes over the North Atlantic: Analysis of precursors and successors. Monthly weather review, 118(10), pp.2056-2081.

1260   Verhulst, A., 2002. The carolingian economy. Cambridge University Press.

Villumsen, T. 2016. Jernaldergården på Grytting. Gårdsbosættelse i 500 år i romertid og folkevandringstid. In I. M. Gundersen (Ed.), Gård og utmark i Gudbrandsdalen : arkeologiske undersøkelser i Fron 2011-2012 (pp. 166-180). Kristiansand: Portal forlag.

Wagner, D. M., Klunk, J., Harbeck, M., Devault, A., Waglechner, N., Sahl, J. W., ... & Poinar, H.
1265   (2014). Yersinia pestis and the Plague of Justinian 541–543 AD: a genomic analysis. The Lancet infectious diseases, 14(4), 319-326.

Welinder, S., 1975. Prehistoric agriculture in Eastern Middle Sweden: a model for food production, population growth, agricultural innovations, and ecological limitations in prehistoric Eastern Middle Sweden 4000 BC-AD 1000 (No. 4). Liberlaromedel.

1270   Westling, S., & Jensen, C. E. 2020. Indications of rye (Secale cereale) cultivation from 7th century south-western Norway. In R. Cappers, W. Kirleis, W. Out, & M. Schepers (Eds.), Archaeobotanical studies of past plant cultivation in northern Europe (pp. 83-100). Groningen: Barkhuis Publishing.

Westling, S., Fredh, E. D., Lagerås, P., & Oma, K. A. 2022. Agricultural Resilience during the 6th Century Crisis: Exploring Strategies and Adaptations Using Plant-Macrofossil Data from Hove-Sørbø
1275   and Forsandmoen in Southwestern Norway. Norwegian Archaeological Review, 1-26. doi:10.1080/00293652.2022.2071331

Wickham, H., 2016. ggplot2: elegant graphics for data analysis. springer.

Wickham, H., Averick, M., Bryan, J., Chang, W., McGowan, L.D.A., François, R., Grolemund, G., Hayes, A., Henry, L., Hester, J. and Kuhn, M., 2019. Welcome to the Tidyverse. Journal of open
1280   source software, 4(43), p.1686.

Wieckowska-Lüth, M., Kirleis, W. and Doerfler, W., 2017. Holocene history of landscape development in the catchment of Lake Skogstjern, southeastern Norway, based on a high-resolution multi-proxy record. The Holocene, 27(12), pp.1928-1947.

Zambri, B., LeGrande, A. N., Robock, A., & Slawinska, J. (2017). Northern Hemisphere winter
1285   warming and summer monsoon reduction after volcanic eruptions over the last millennium. *Journal of Geophysical Research: Atmospheres*, *122*(15), 7971-7989.

Zambri, B., Robock, A., Mills, M.J. and Schmidt, A., 2019. Modeling the 1783–1784 Laki eruption in Iceland: 2. Climate impacts. Journal of Geophysical Research: Atmospheres, 124(13), pp.6770-6790.

1290   Zhong, Y., Miller, G.H., Otto-Bliesner, B.L., Holland, M.M., Bailey, D.A., Schneider, D.P. and Geirsdottir, A., 2011. Centennial-scale climate change from decadally-paced explosive volcanism: a coupled sea ice-ocean mechanism. Climate Dynamics, 37(11), pp.2373-2387.

Åssveen, M., & Abrahamsen, U. (1999). Varmesum for sorter og arter av korn. Grønn forskning(2), 55-59.

1295 **Appendix A**

A1. Climate model simulations
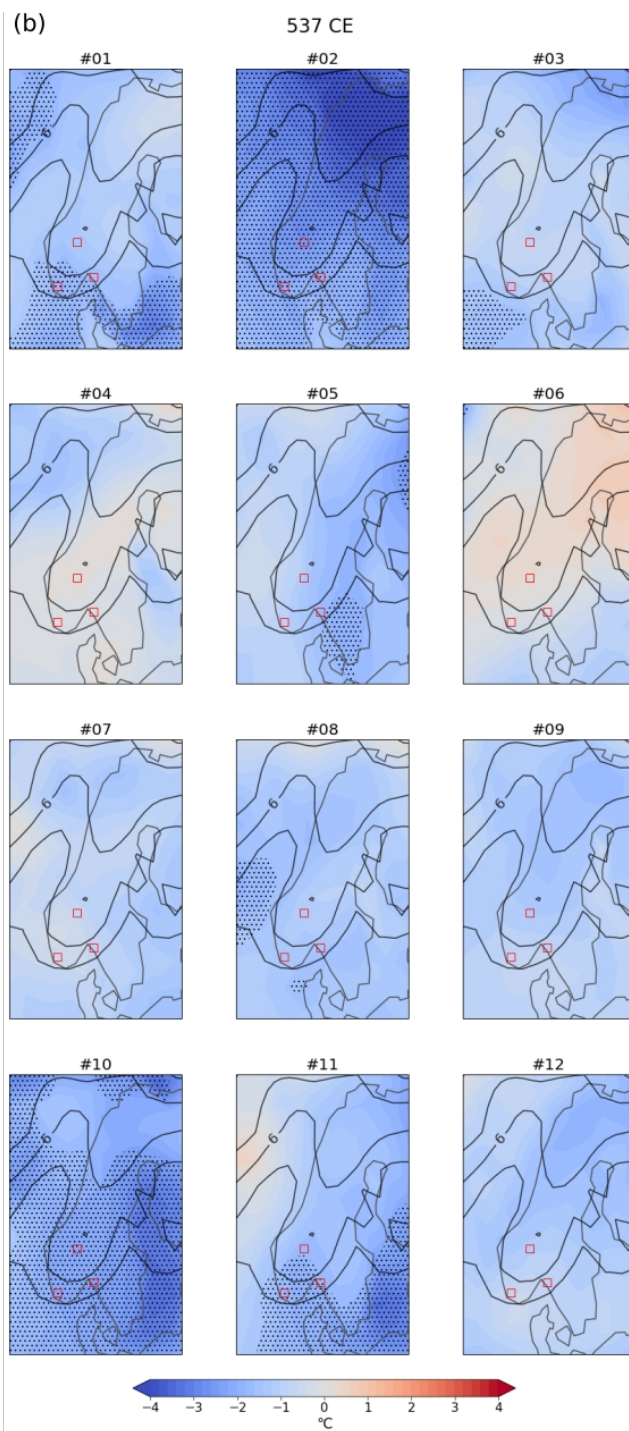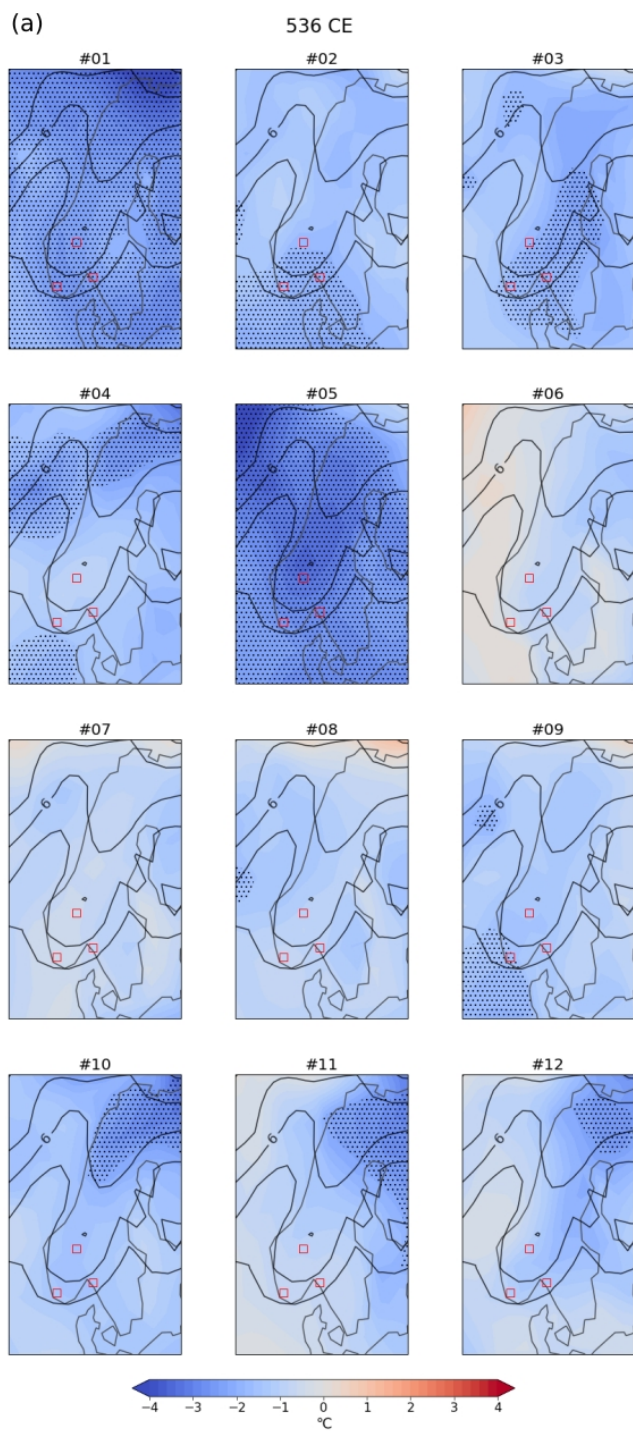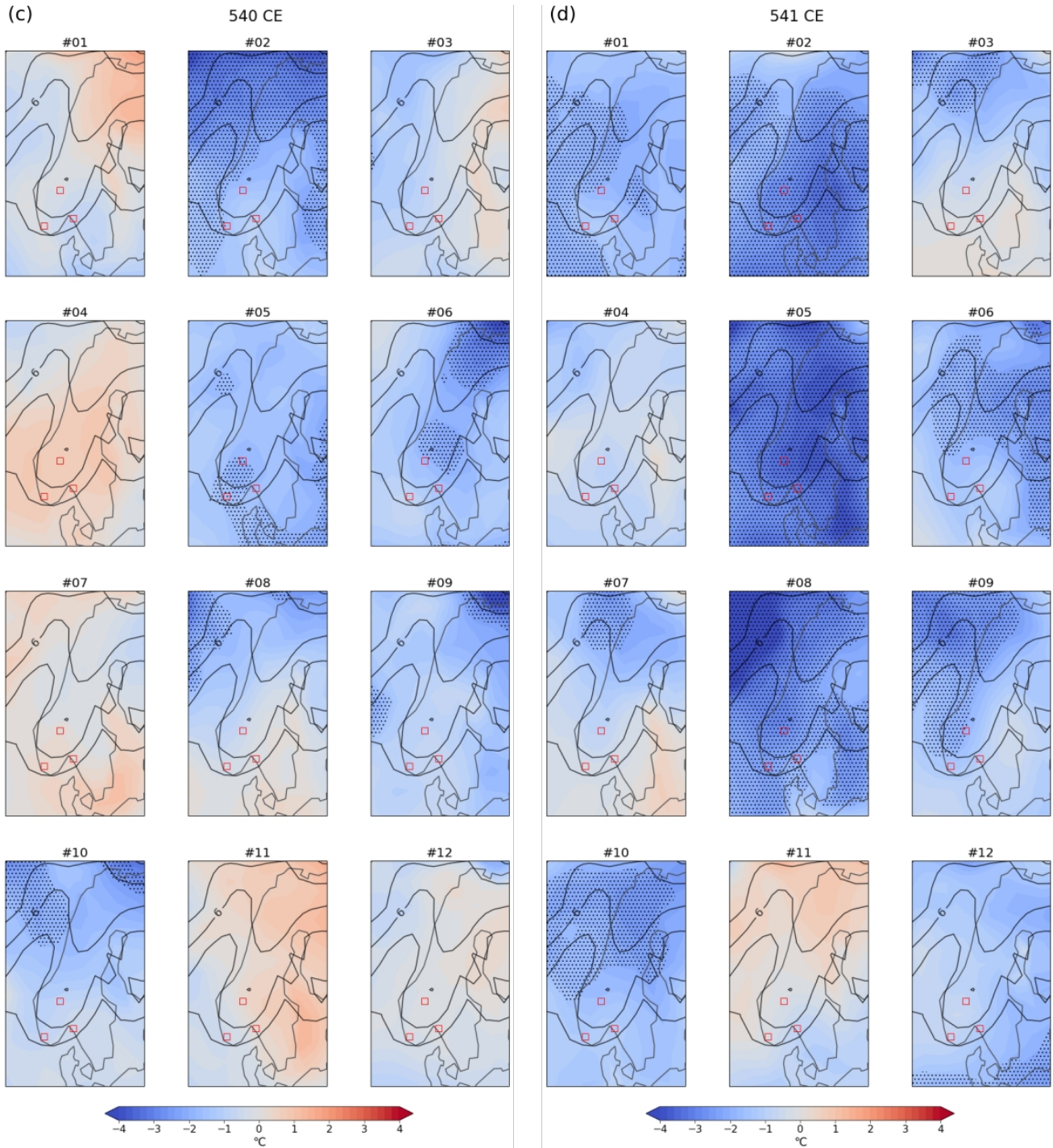
Figure A1. 2m air temperature anomaly for the individual ensemble members of a) 536 CE, b) 537 CE, c) 540 CE, and d) 541 CE. Anomalies are calculated with respect to the 1-1850 CE climatology in contours (1 °C intervals). The red squares indicate the areas used for the growing degree day calculations. The 2σ significant level is stippled.

1300
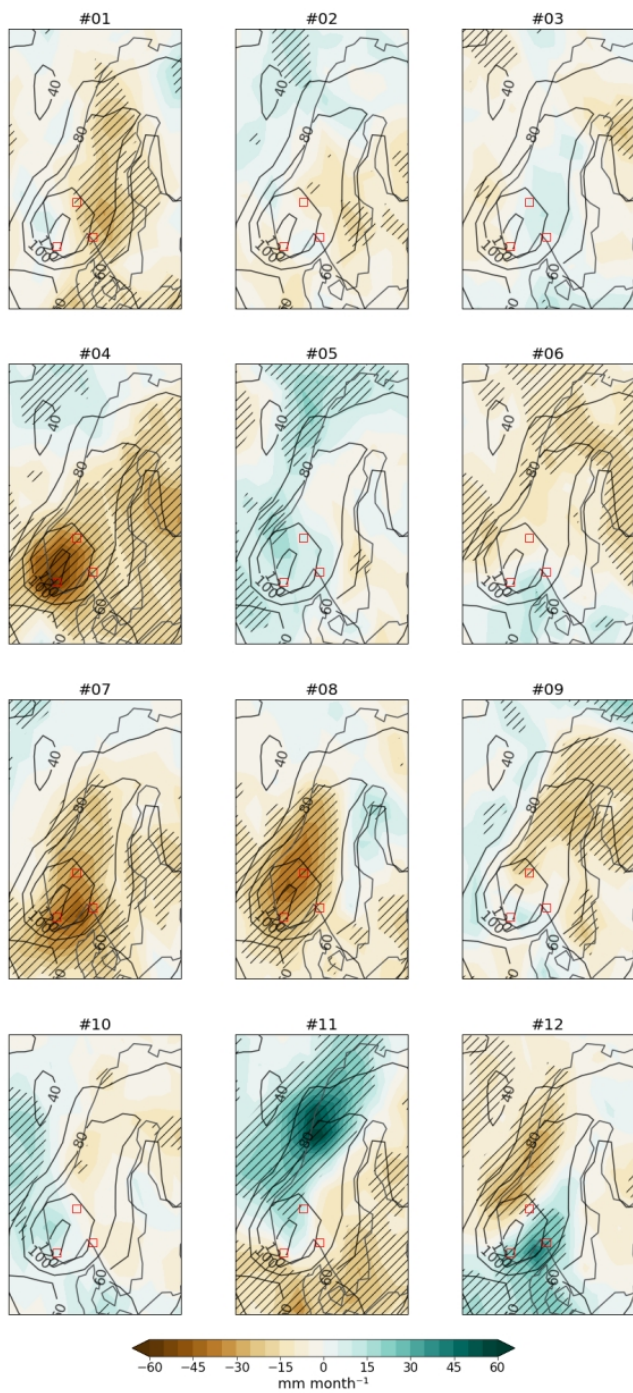
(a) 536 CE   (b) 537 CE
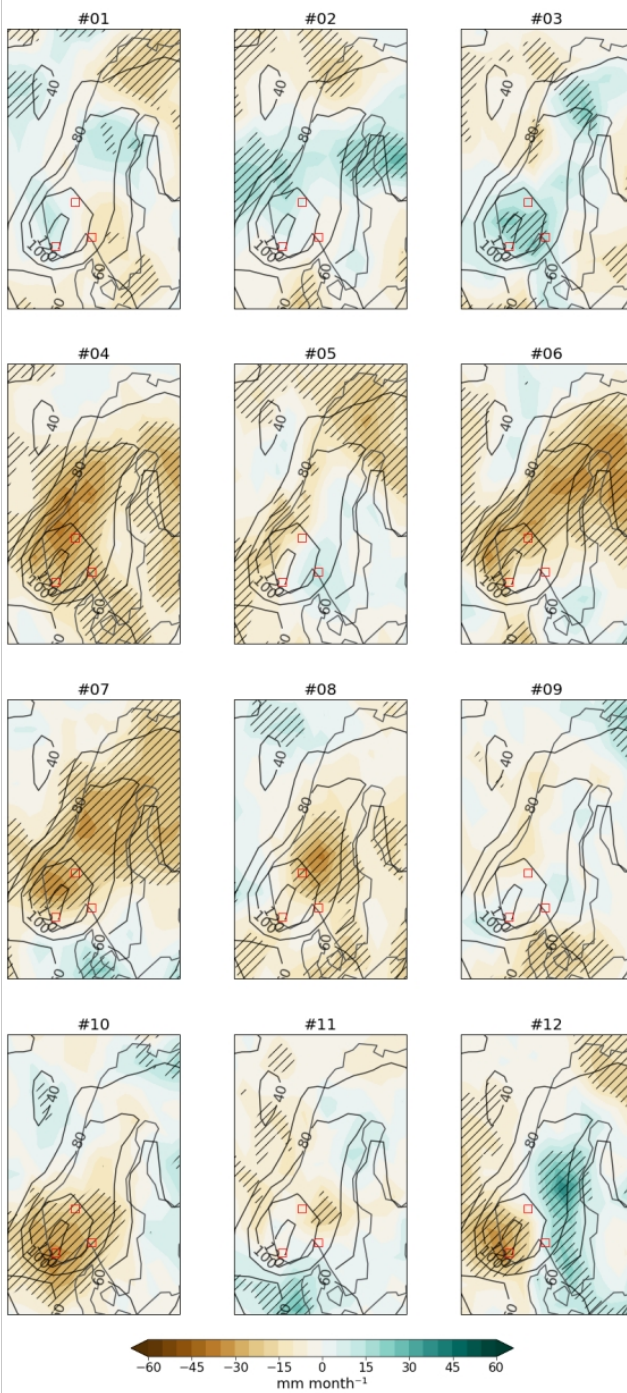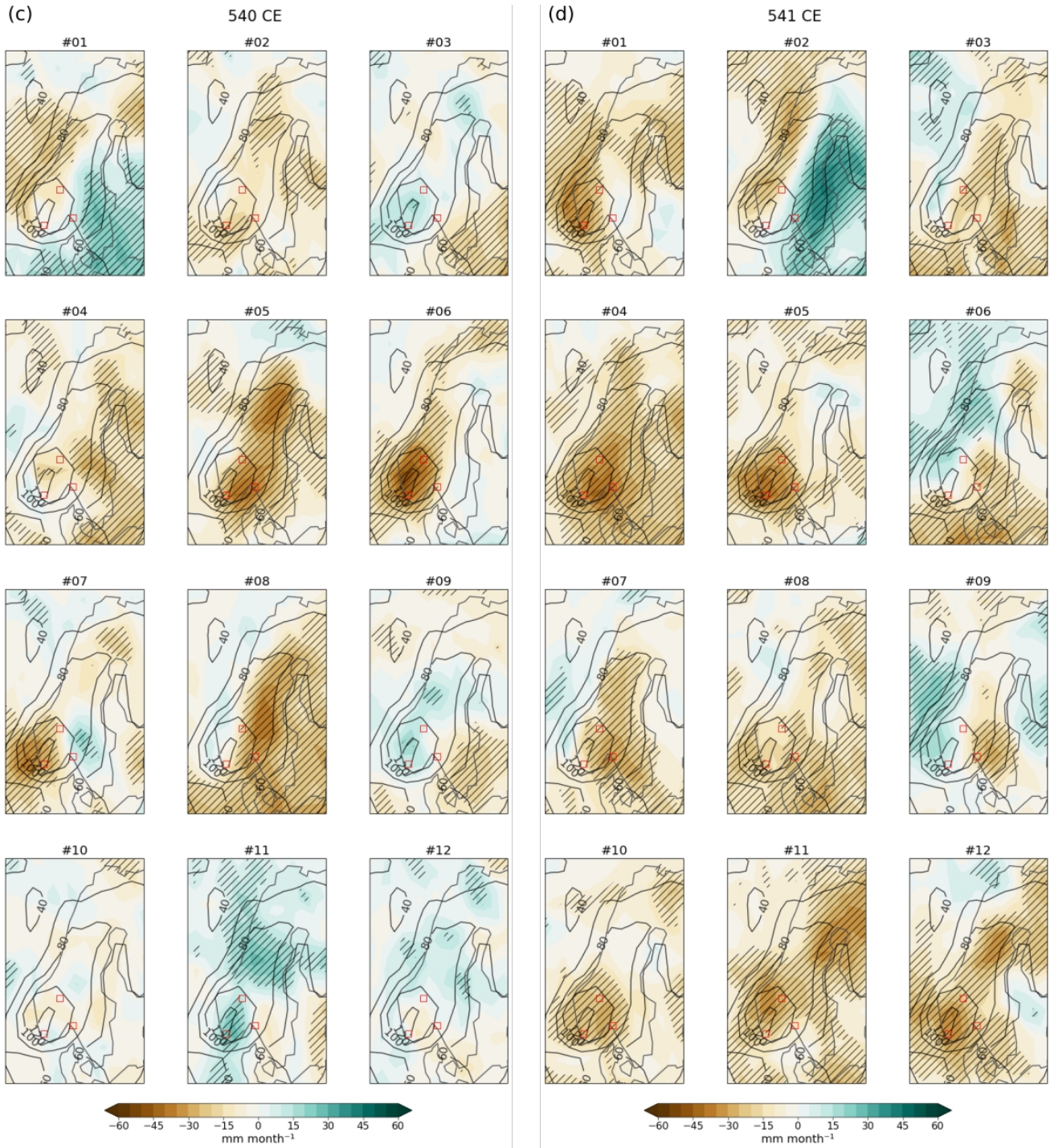
Figure A2. As Fig. A1 for precipitation anomaly. The 1σ significant areas are hatched. Contours are shown for 20 mm month⁻¹ intervals.
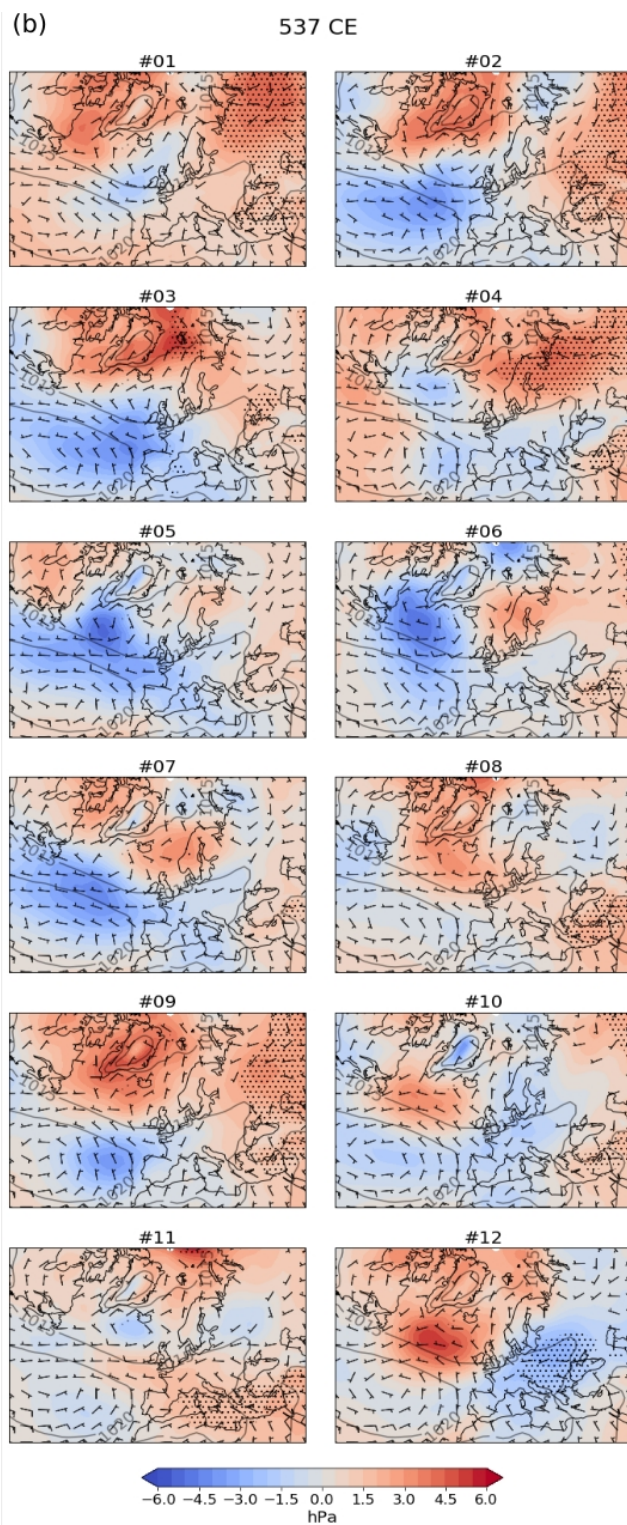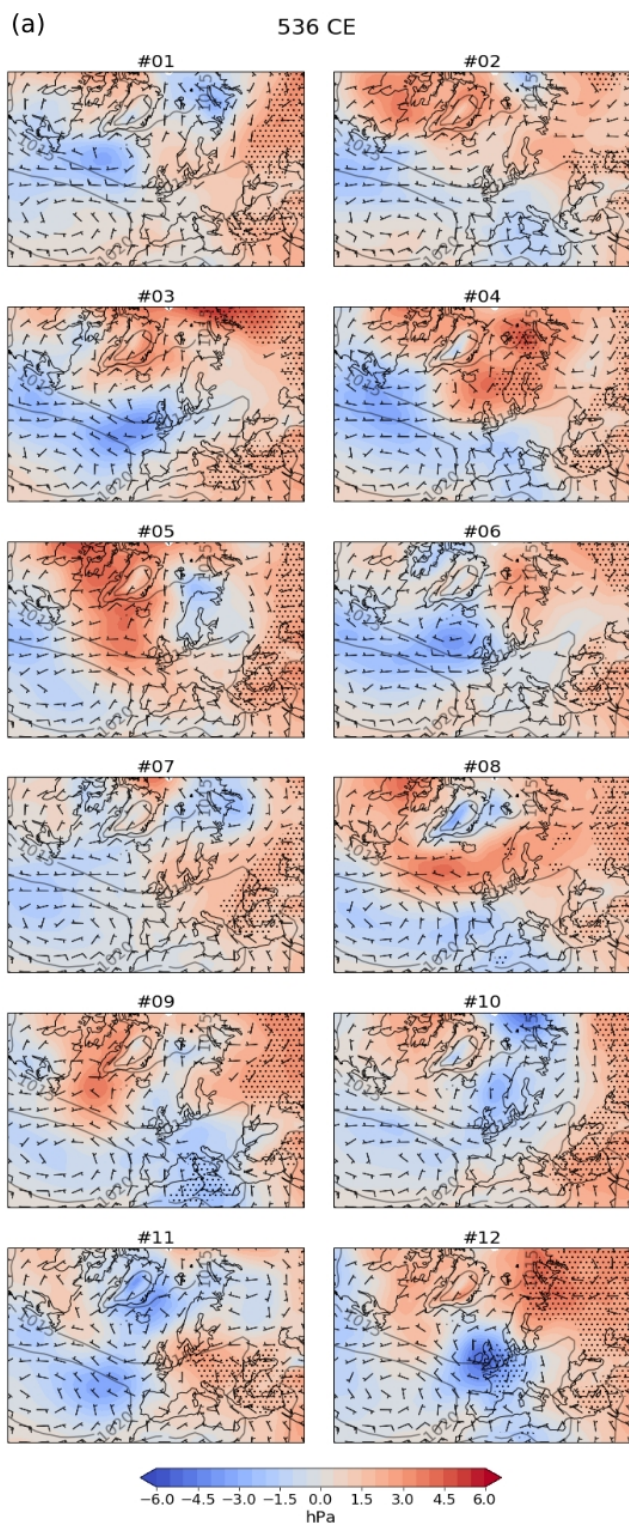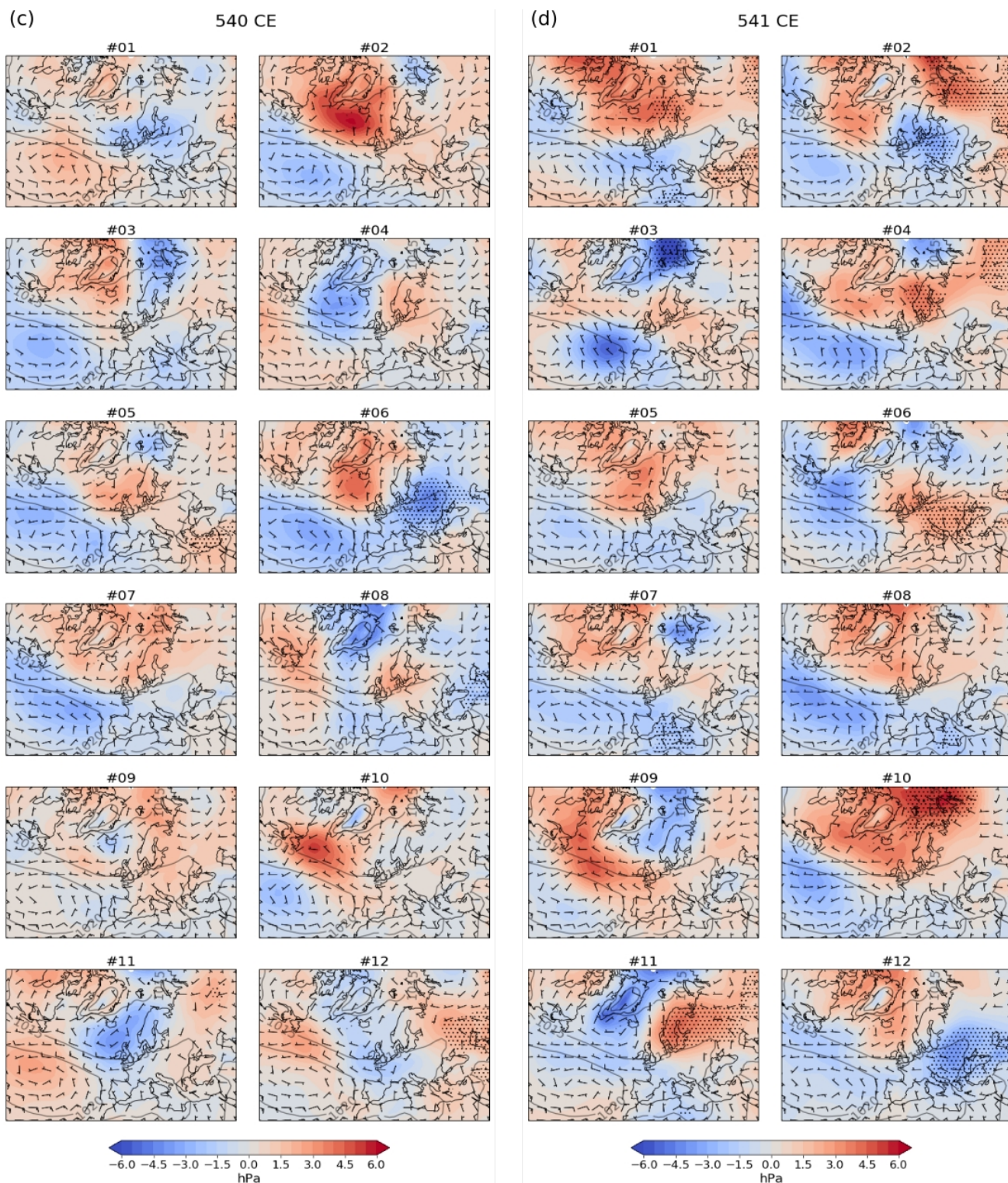
Figure A3. As Fig. A1 for sea level pressure (SLP) anomaly and absolute wind. SLP contours and wind barbs are shown for 5 hPa and 1, 5 and 10 m/s intervals, respectively.

1305

A1.1. Atmospheric circulation analyses

Analysing the general atmospheric circulation patterns by using EOF analysis, for the April-September growing season from the past2k run #1 (Fig. A4b), reveals the growing season
1310 atmospheric circulation anomaly patterns to be a combination of the winter and summer modes (not shown here), with a similar distribution of high and low pressure centres as in winter, but not as concentrated. The four leading modes are a NAO+ like pattern with 38%, a NAO- like pattern with 8%, a weaker NAO+ like pattern with 7% and a blocking like pattern with the high pressure over the Kara sea with 6%.

1315 Van Dijk et al. (2022) showed a significant SLP anomaly, with an increase over the high-latitudes and a decrease over the mid-latitudes two years after the large eruptions that occurred during 520-680 CE for JJA, whereas the DJF signal is not significant due to high internal variability in the winter months. These SLP patterns are similar as we find in this study for the mean growing season AMJJAS (Fig. 4), with a higher pressure over the high-latitudes and land, and a decrease in pressure
1320 over the mid-latitudes for the NH. In addition, van Dijk et al. (2022) calculated the NAO index for the DJF SLP, resulting in a positive NAO response the first year after the eruption for three out of four eruptions, followed by a more neutral or even a negative NAO response in the year after.

From the SLP anomaly for AMJJAS in Fig. 4, it can be seen that the atmospheric circulation response over Scandinavia is significant for the ensemble mean growing season for 536-560 CE, but
1325 not two years after the 536 and 540 eruptions. The different patterns in the precipitation and SLP anomalies are cancelled out in the ensemble mean, resulting in a weak volcanic signal. Even though the 536-560 CE mean gives a significant positive anomaly for Scandinavia (Fig. 4a), the individual runs highlight differences in the regional responses as possible realisations.

NAO+

Mode 1 - 50%

Scandinavian Blocking

Mode 2 - 11%

NAO-

Mode 3 - 10%

Atlantic ridge

Mode 4 - 6%

-400 -300 -200 -100 0 100 200 300
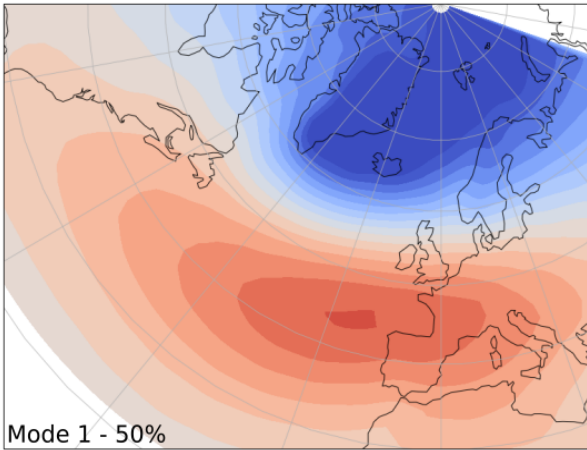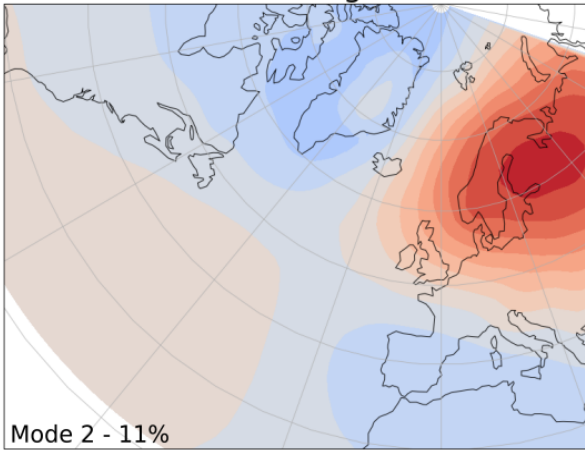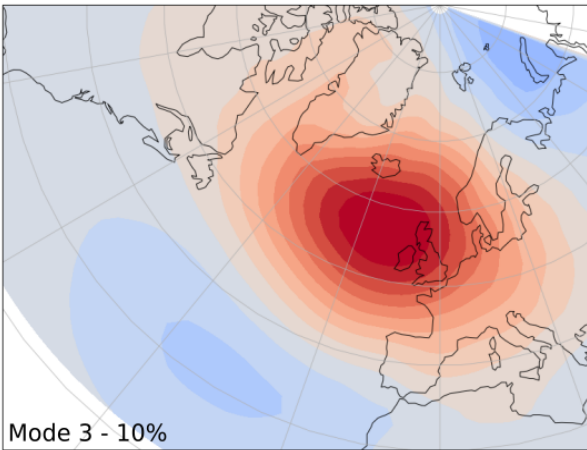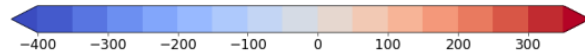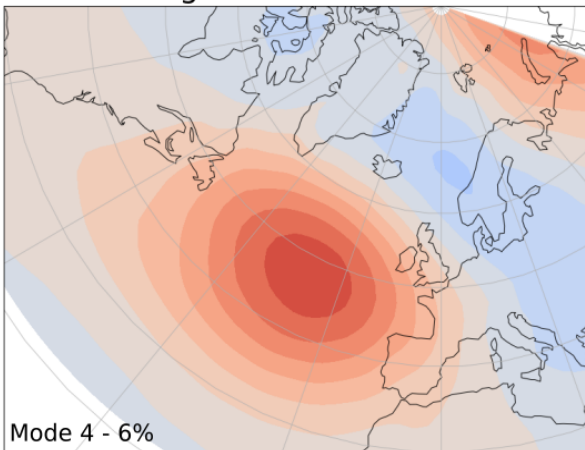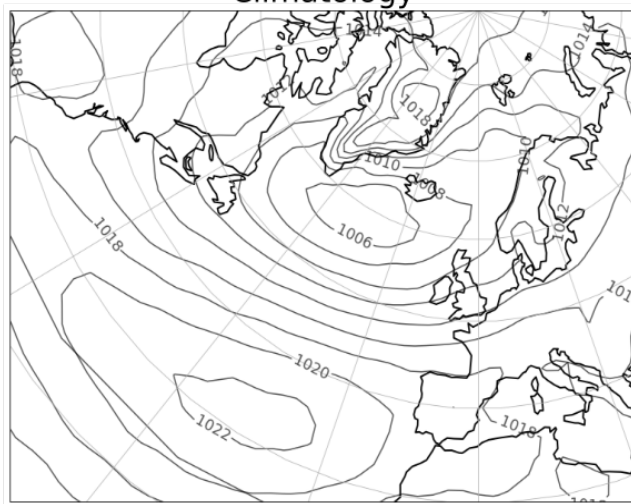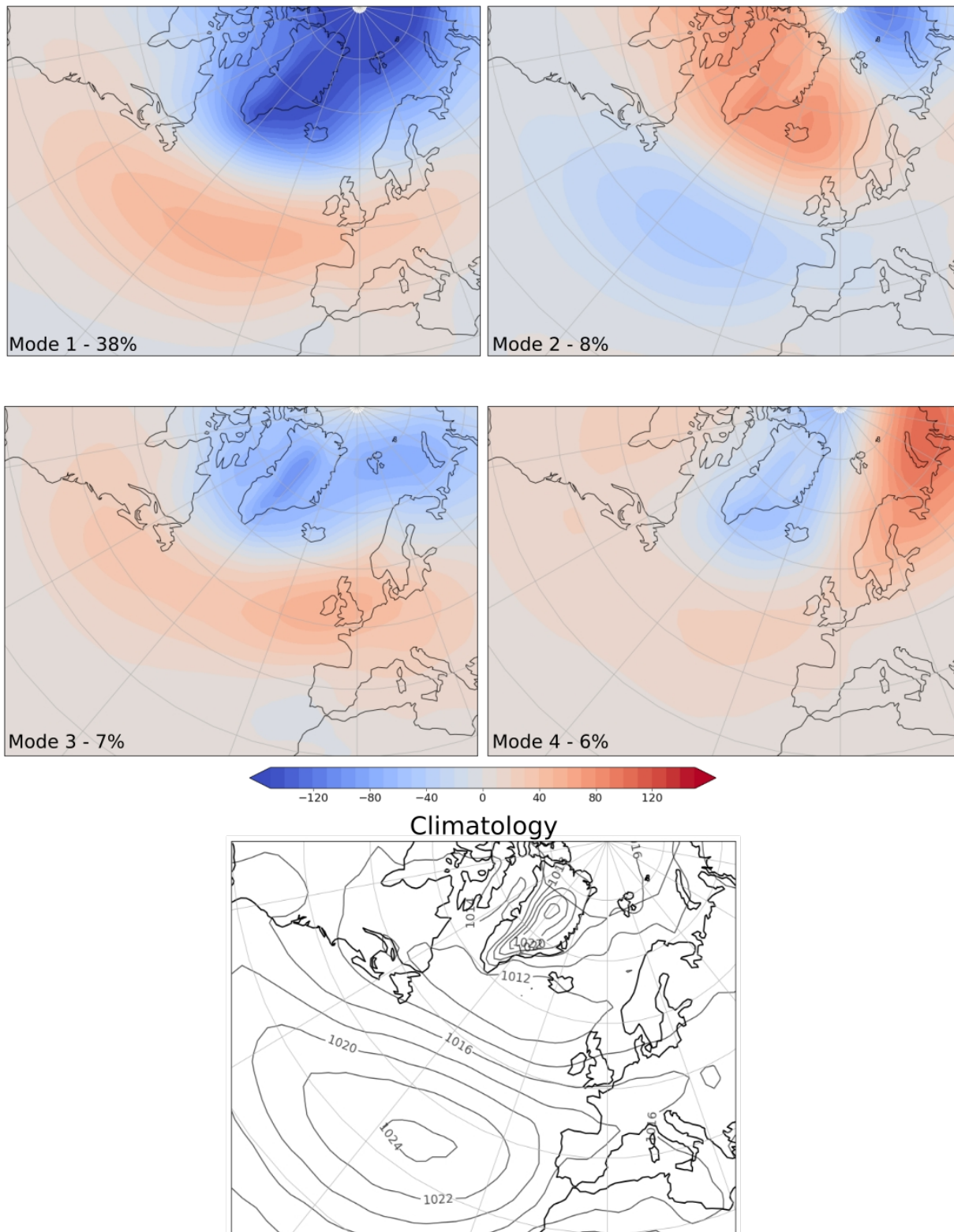
Climatology

Figure A4. The SLP EOF first four modes of atmospheric circulation patterns for the past2k #1 for a) DJF (see also van Dijk et al., 2022) and b) the mean growing season (AMJJAS) during 1-1850 CE. The SLP climatology for 1-1850 CE is given in the lowest panel; contours are given in 2 hPa intervals.

A2. Study sites
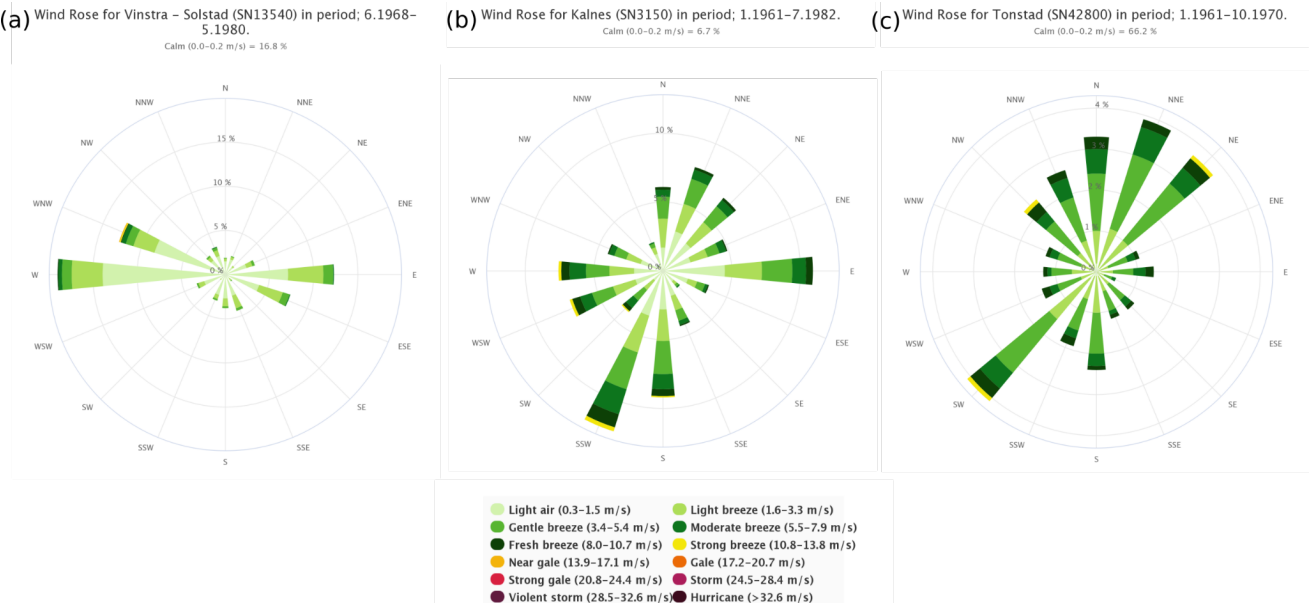
Figure A5. Annual mean 10m wind data for 1961-1990 (eklima.no) for the a) Fron, b) Sarpsborg and c) Høgsfjorden areas. Data is taken from the nearest meteorological station with the same valley orientation as the study area.

A3. Pollen data

A3.1. Chronology

The uncalibrated and calibrated radiocarbon ages of Haraldstadmyr peat sequence are presented in Table A1. An age-depth model was generated based on these 9 radiocarbon ages, as presented in Fig. A6. The top of the core, i.e. 0 cm, was incorporated in the construction of the age-depth model as the year of the coring in 2018 CE.

The age-depth model indicates that the peat sequence approximately covers the last 4000 years. The peat accumulations vary throughout the core. From 0-45 cm, the accumulation rate measures 0.36 mm/yr. The accumulation rate increases from 45-109.5 cm to 1.18 mm/yr. From 109.5-275.5 cm, the mean accumulation rate measures 0.52 mm/yr.

Table A1: Radiocarbon ages for Haraldstadmyr peat sequence.

Lab number	Core depth (cm)	¹⁴C age BP	Min. age (cal BP)	Max. age (cal BP)	Min. age (cal BCE/CE)	Max. age (cal. BCE/CE)	Mean age (cal. BCE/CE)
LuS-16754	20	520 ±30	263	531	1687	1419	1582
Ua-61355	45	866 ±28	573	770	1377	1180	1246
β-508936	91.5	1040 ±30	980	1161	970	789	896
β-508937	102.5	1230 ±30	1101	1240	849	710	785
β-508938	109.5	1260 ±30	1192	1293	758	657	703
Ua-61356	123.5	1612 ±28	1428	1676	522	274	427
LuS-16755	150	2595 ±35	2392	2760	-422	-810	-655
LuS-16756	203	3820 ±35	3997	4333	-2047	-2383	-2219
LuS-16757	275.5	5155 ±40	5677	5985	-3727	-4035	-3891
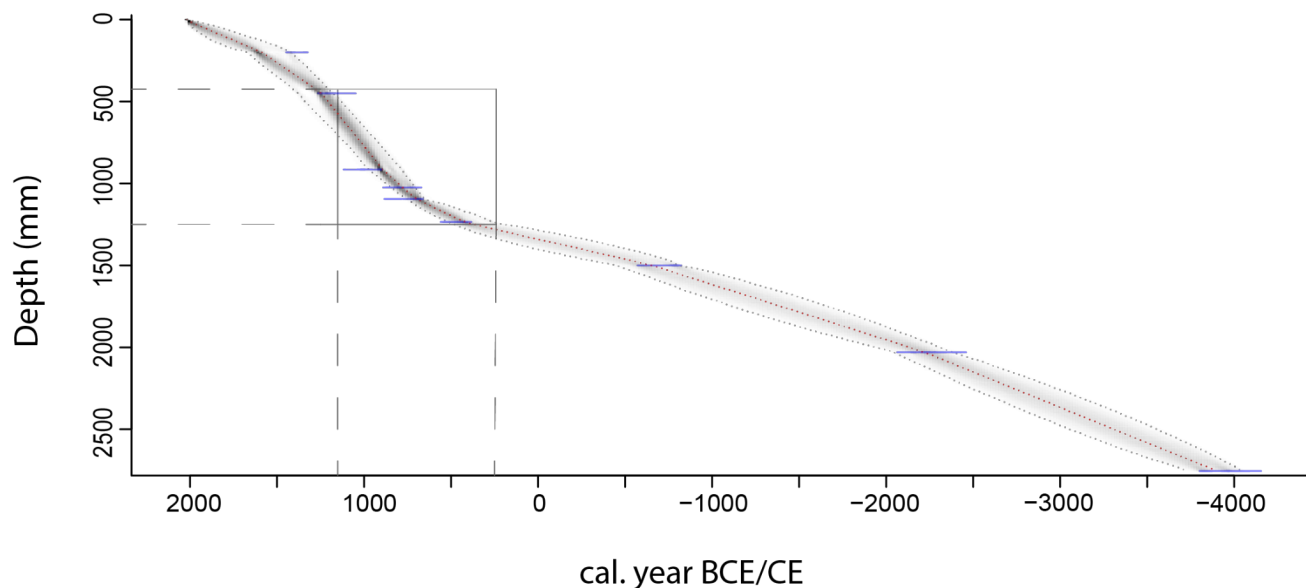
Figure A6: Age-depth model of Haraldstadmyr peat sequence, represented with the RBacon package. The section in the rectangle indicates the study period 250-1150 CE.

The uncalibrated and calibrated radiocarbon ages of Ulbergmyr peat sequence are presented in
1350   Table A2. Sample LuS-15686 was discarded, as this sample was found to be older than the sample taken at 108 cm. The year of coring was excluded during the construction of the age-depth model. As a result, the age-depth model (Fig. A7) was generated based on 5 radiocarbon ages in total.

Table A2: Radiocarbon ages for Ulbergmyr peat sequence.

Lab number	Core depth (cm)	¹⁴C age BP	Min. age (cal BP)	Max. age (cal BP)	Min. age (cal BCE/CE)	Max. age (cal. BCE/CE)	Mean age (cal. BCE/CE)
Ua-67047	35	1191 ±29	1229	1024	721	926	822
LuS-15685	52	1455 ±35	1363	1188	587	762	637
LuS-15686	92	1720 ±35					
LuS-15687	108	1715 ±35	1734	1588	216	362	278
LuS-14936	125	1880 ±35	1904	1736	46	214	139
LuS-14935	495	4620 ±40	5542	5115	-3592	-3165	-3423
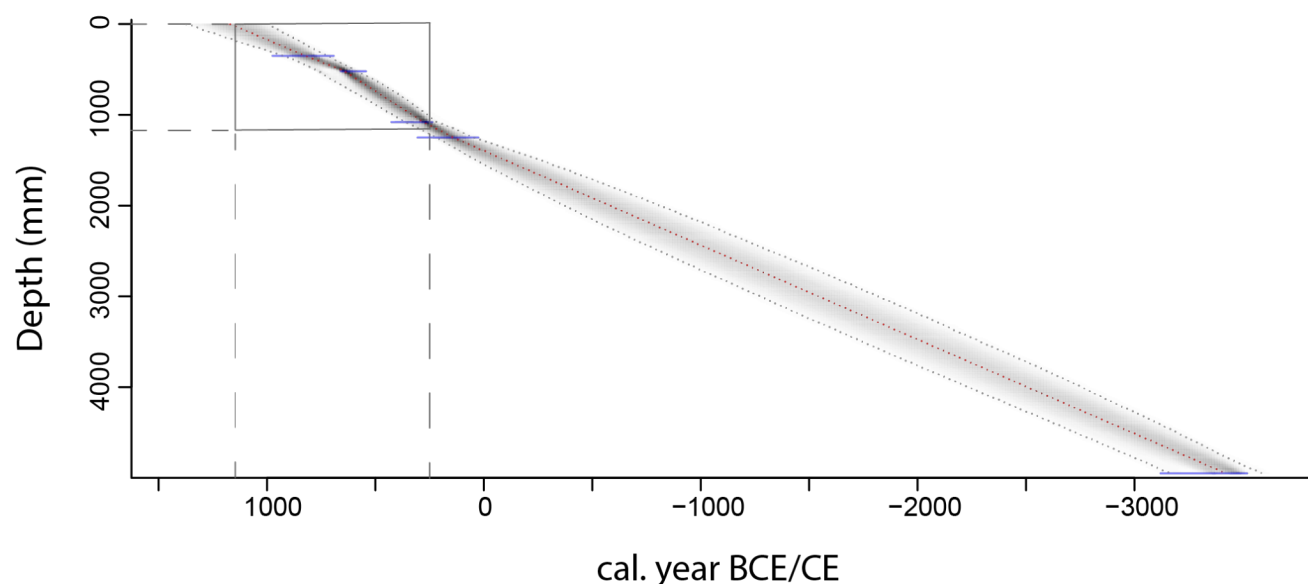
Figure A7: Age-depth model Ulbergmyr peat sequence, represented with the RBacon package. The
1355   **section in the rectangle indicates the study period 250-1150 CE.**

The chronology of Ulbergmyr peat sequence approximately covers the last 3500 years. However, as
the bottom of the bog was not reached during the coring, the complete chronology of the bog most
likely dates back even further. From 35-52 cm, the mean accumulation measures 0.92 mm/yr. The
mean accumulation rate is relatively higher from 52-108 cm in comparison to the rest of the core,
1360   namely 1.56 mm/yr. The age-depth model is linear from 108-495 cm, with a mean accumulation rate
of 1.05 mm/yr.

The radiocarbon ages of Åsheimmyr peat sequence are listed in Table A3. Sample Ua-72109 was
discarded, as this radiocarbon age was found to be too old (Selsing, Lillehammer and Griffin, 1999).

The year of the coring was excluded during the construction of the age-depth model.

1365 **Table A3: Radiocarbon ages for Åsheim peat sequence**

Lab number	Core depth (cm)	¹⁴C age BP	Min. age (cal BP)	Max. age (cal BP)	Min. age (cal BCE/CE)	Max. age (cal. BCE/CE)	Mean age (cal. BCE/CE)
	240	312 ±30	419	807	1531	1143	1409
Ua-72108	320	1147 ±28	966	1172	984	778	898
Ua-72109	360	1664 ±29					
	440	1872 ±31	1730	1988	220	-38	118
Ua-72110	630	3655 ±30	3842	4089	-1892	-2139	-2018
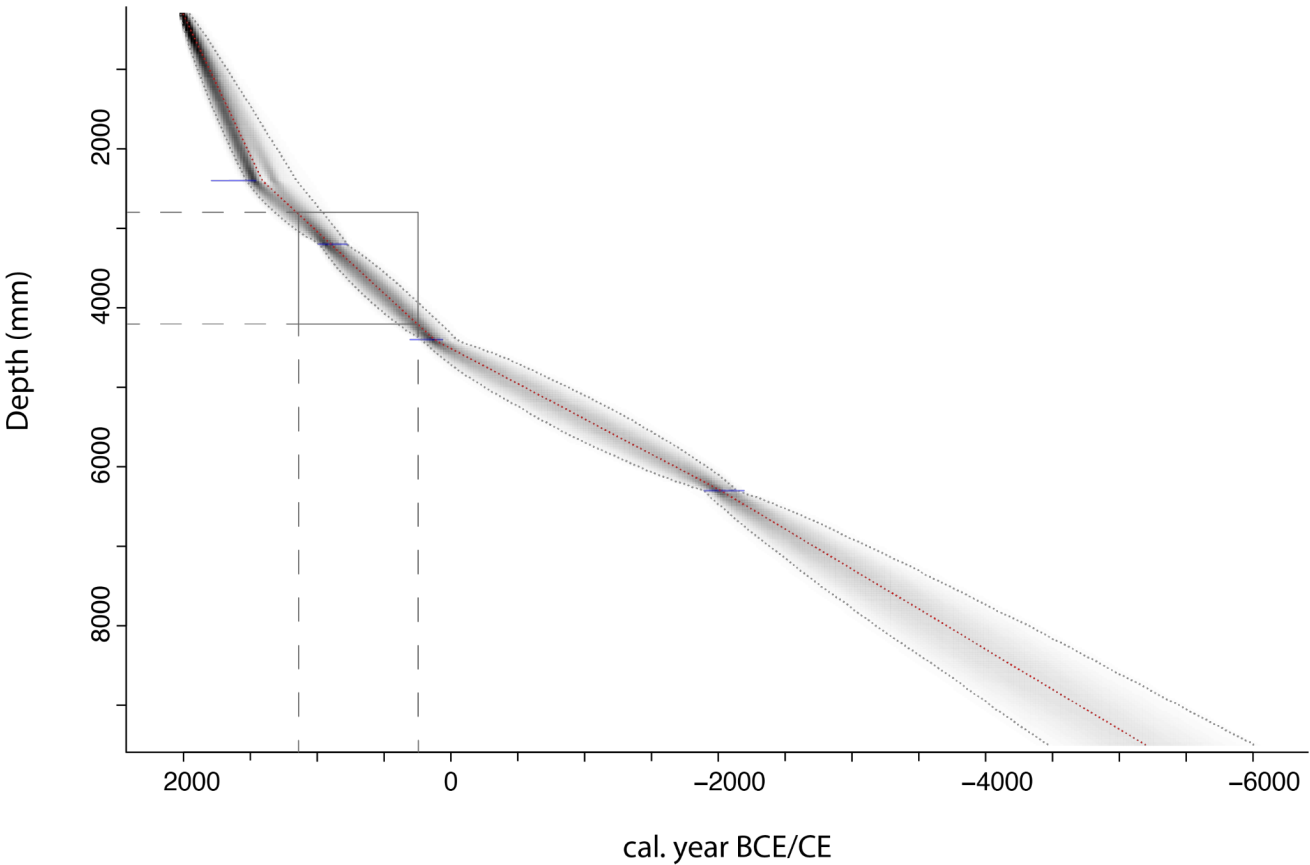
Figure A8: Age-depth model for the Åsheimmyr peat sequence represented with the RBacon package. The section in the rectangle indicates the study period 250-1150 CE.

Åsheimmyr peat sequence covers over 5000 years (Fig. A8). The mean accumulation rate is the highest at the top of the bog, from 30-240 cm, i.e. 3.54 mm/yr, after which the accumulation rate decreases to 1.55 mm/yr from 240-440 cm. The lower part of the peat sequence, from 440-630 cm has a mean accumulation rate of 0.89 mm/yr.

1370
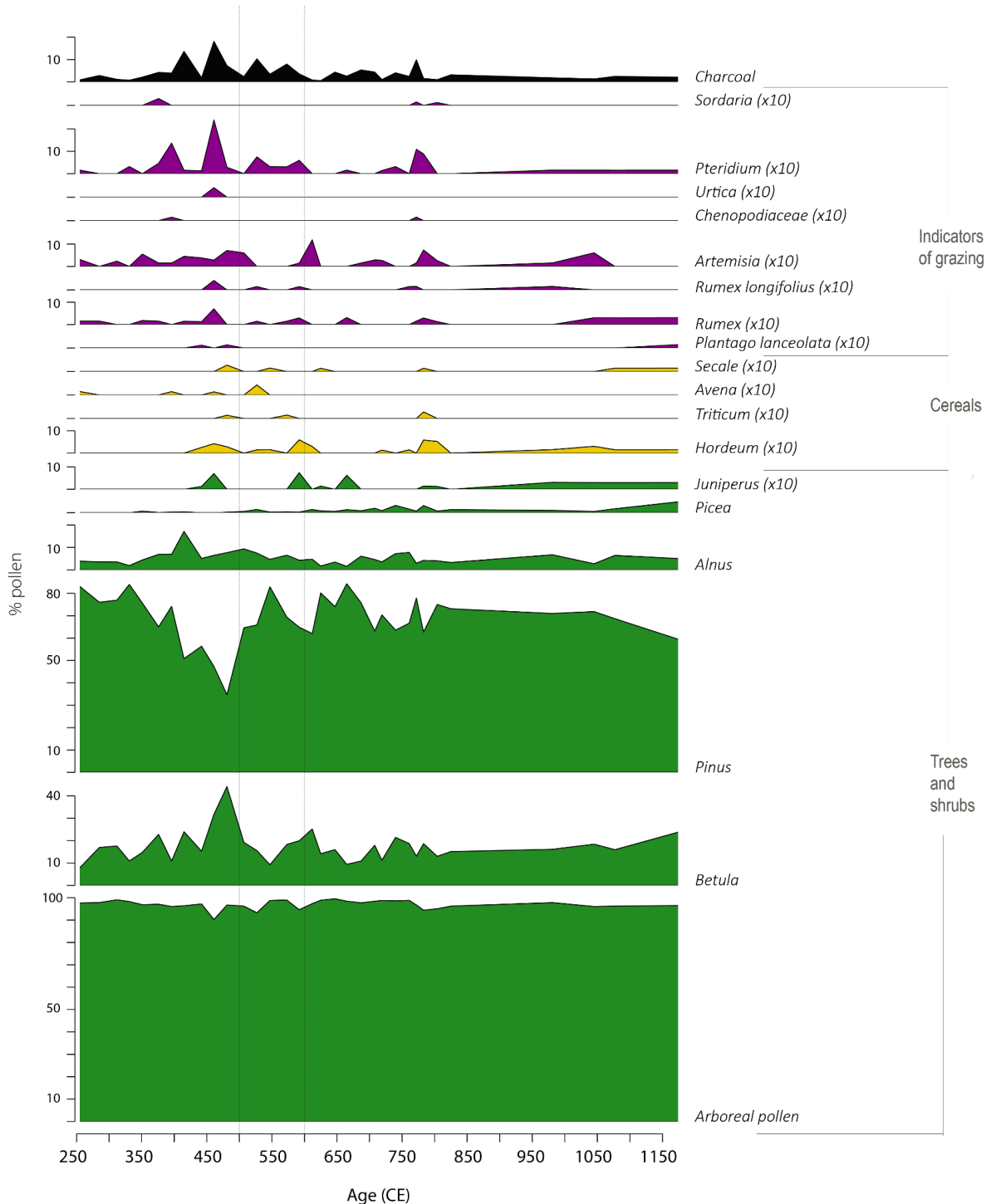
Figure A9. Percentage pollen diagram of Ulbergmyr peat sequence (Fron area), showing a selection of trees, cereals, and other anthropogenic indicators according to cal. age (CE), from 250 BCE to 1150 CE. Pollen types that were multiplied by 10 are indicated with (x10) in the title for each pollen type.

1375   **Percentages of pollen, spores and non- pollen palynomorphs outside the pollen sum (X) are based on (ΣP+X).**

Figure A10. Percentage pollen diagram for Åsheimmyr (Forsand area), showing a selection of trees, cereals, and other anthropogenic indicators according to cal. age (CE), from 250 BCE to 1150 CE. Pollen types that were multiplied by 10 are indicated with (x10) in the title for each pollen type.

1380   **Percentages of pollen, spores and non- pollen palynomorphs outside the pollen sum (X) are based on (ΣP+X).**
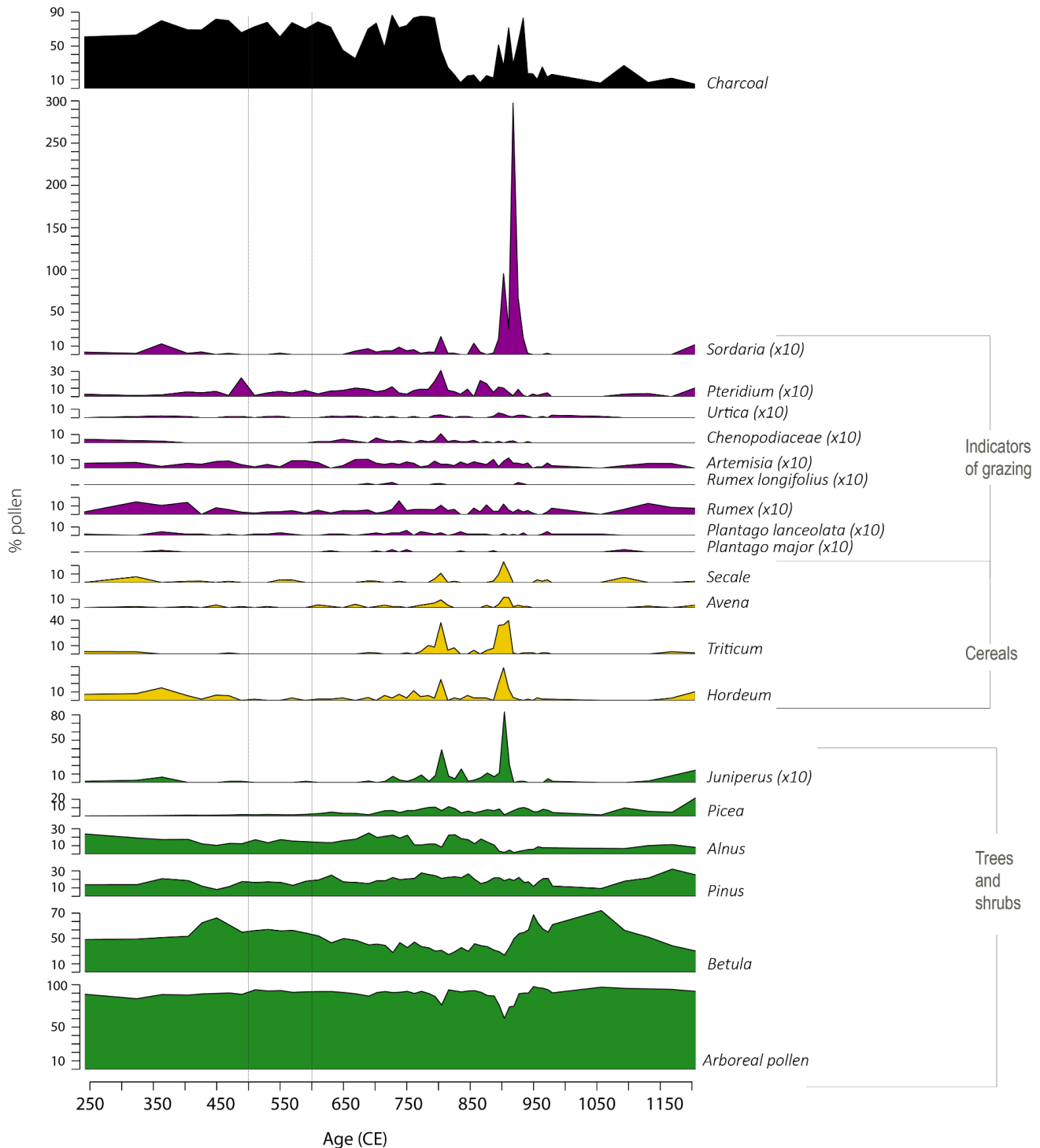
Figure A11. Percentage pollen diagram of Haraldstadmyr peat sequence (Sarpsborg area), showing a selection of trees, cereals, and other anthropogenic indicators according to cal. age (CE), from 250 BCE to 1150 CE. Pollen types that were multiplied by 10 are indicated with (x10) in the title for each pollen type. Percentages of pollen, spores and non- pollen palynomorphs outside the pollen sum (X) are based on (ΣP+X).

1385

Table A4. Information about the proxies and locations marked in Fig. 9.

Location	Coordinates	Type of data	Reference
Tornetrask	68.25° N, 19.6° E	Tree-ring	Grudd, 2008
Northern Scandinavia (NScan)	68° N, 24° E	Tree-ring	Esper et al., 2012
Ulbergmyr, Norway	61.64° N, 9.63° E	Pollen	This study
Åsheimmyr, Norway	58.89° N, 6.22° E	Pollen	This study
Haraldstadmyr, Norway	59.17° N, 11.03° E	Pollen	This study
Forsand, Norway	58.89° N, 6.22° E	Finds of ergot	Løken, 2020
Medelpad, Sweden	62.42° N, 17.05° E	Pollen showing decline agriculture mid-6th century	Pedersen and Widgren, 2011
Blekinge, Sweden	56.25° N, 15.02° E	Pollen showing decline agriculture mid-6th century	Pedersen and Widgren, 2011
Gotland, Sweden	57.45° N, 18.97° E	Pollen showing decline agriculture mid-6th century	Pedersen and Widgren, 2011
Forsand, Norway	58.89° N, 6.22° E	Evidence for site abandonment	Løken, 2020
Fron	61.64° N, 9.63° E	Evidence for site abandonment	Gundersen, 2021
Bjørnstad, Tune	59.17° N, 11.03° E	Evidence for site abandonment	Bårdseth, 2007; Rødsrud, 2007
Öland, Sweden	56.70° N, 16.60° E	Pollen showing decline agriculture mid-6th century	Pedersen and Widgren, 2011
Gotland, Sweden	57.62° N, 18.55° E	Evidence for site abandonment	Gräslund and Price, 2012
Southern Norway	58.50° N, 8.38° E	Evidence for site abandonment	Solberg, 2000
Southwest Norway	59.43° N, 5.58° E	Evidence for site abandonment	Solberg, 2000
Mälaren valley, Sweden	59.72° N, 16.20° E	Evidence for site abandonment	Löwenborg, 2012

Levänluhta, Finland	62.9° N, 22.4° E	Versatile livelihood	Oinonen et al., 2020
Fyn, Denmark	55.3° N, 10.4° E	reorganisation	Hansen, 2016